Engineered sensor bacteria evolve master-level gameplay through accelerated adaptation

Satya Prakash[1], Adrian Racovita[2], Clenira Varela[1], Mark Walsh[1], Roberto Galizi[3], Mark Isalan[4], Alfonso Jaramillo[1,2†]

[1] Warwick Integrative Synthetic Biology Centre and School of Life Sciences, University of Warwick, Coventry CV4 7AL, UK.

[2] *De novo* Synthetic Biology Lab, i2SysBio, CSIC-University of Valencia, Paterna, Spain. Alfonso.Jaramillo@csic.es.

[3] Centre for Applied Entomology and Parasitology, School of Life Sciences, Keele University, Keele ST5 5BG, UK.

[4] Department of Life Sciences, Imperial College London, London SW7 2AZ, UK.

[†] Corresponding author and lead contact: Prof. Alfonso Jaramillo. *De novo* Synthetic Biology Lab, i2SysBio, CSIC-University of Valencia, Paterna, Spain. Alfonso.Jaramillo@csic.es.

Abstract

Gene circuits enable cells to make decisions by controlling the expression of genes in reaction to specific environmental factors[1]. These circuits can be designed to encode logical operations[2-7], but implementation of more complex algorithms has proved more challenging. Directed evolution optimizes gene circuits[8] without the need for design knowledge[9], but adjusting multiple genes and conditions[10] in genotype searches poses challenges[11]. Here we show a multicellular sensor system, AdaptoCells, in Escherichia coli, that can evolve complex behavior through an accelerated adaptation to chemical environments. AdaptoCells recognize chemical patterns and act as a decision-making system. Using an iterative improvement method, we demonstrate that the AdaptoCells can evolve to achieve mastery in the game of tic-tac-toe, demonstrating an unprecedented level of complexity for engineered living cells. We provide an effective and straightforward way to encode complexity in gene circuits, allowing for fast adaptation in response to dynamic environments and leading to optimal decisions.

Keywords: Multicellular gene circuits, synthetic biology, directed evolution, heteroplasmy system, sub-lethal antibiotic selections, tic-tac-toe, adaptation decision-making.

Gene circuits are a fundamental tool in biotechnology, allowing regulation of gene expression and enabling organisms to respond to environmental changes using chemical sensors. However, despite progress in gene circuit design[12], it remains a challenge to create circuits that can make complex decisions, such as playing an expert strategy in a board game. This requires a decision-making algorithm based on environmental conditions, represented by chemical sensors and a truth table that determines the optimal move. Conventional gene circuits struggle to encode the truth table of even the simplest board games, due to the need for numerous logic gates and transcription factors.

A promising approach to engineering complex gene circuits is the use of multicellular gene circuits[3, 4], which allow for communication between cells. This approach involves dividing genes into separate cells within a population, resulting in the collective behavior of the population resembling that of a single-cell gene circuit. By using this divide-and-conquer strategy, it is possible to design more complex gene circuits that mimic internal gene-gene regulations through the engineering of orthogonal cell-cell communications. However, despite this potential, implementing gene-gene regulations at the multicellular level remains a challenging problem due to the limited number of independent chemical communication channels available and the complexity involved in connecting multiple logic gates through internal gene-gene interactions. So far, it has only been achieved for a limited number of independent chemical communication channels[13], which is not enough to support the design of advanced decision-making that requires multiple logic gates to be connected through internal gene-gene interactions. This limitation hinders the assembly of the numerous logic gates needed for complex truth tables. For example, an implementation of an expert tic-tac-toe player using DNA computing and logic gates required 128 three-input gates[14].

Analog gene circuits[15, 16] use continuous signals to perform complex algorithms, monitoring the environment, regulating gene expression, and processing signals. To make these circuits more versatile and enable decision-making, discretizing output genes transforms the

continuous output into a discrete or digital signal by dividing it into distinct levels. Although analog gene circuits with discretized output can be useful, gene circuits with digital behavior are more commonly used. The "winner-take-all" strategy is a powerful discretization method that enables decision-making based on the gene circuit with the strongest phenotype[17]. This approach provides several advantages over other discretization methods, as it considers the relative strengths of multiple signals to decide, rather than relying on a single threshold value. However, designing analog gene circuits for decision-making can still present challenges due to their sensitivity to gene expression levels of each transcription factor. Automated design methods, such as computational design, have aided the engineering of analog gene circuits for biological adaptive behaviors[18], but they have not yet successfully implemented advanced decision-making[19, 20]. Nonetheless, this has been achieved artificially using physical and chemical systems by engineering memory units with neuromorphic computing capabilities[21-27].

Darwinian directed evolution's trial-and-error approach - that generates genetic variations like mutations or recombination - has proven to be a challenge for engineering complex gene circuits in living cells. The lack of continuity in phenotype space, slow pace, and difficulty in covering the vast genetic space of multi-gene circuits limit its effectiveness. Furthermore, the multi-objective selection process for truth tables in gene circuits implementing logic gates often involves complex methods and high concentrations of antibiotics, reducing genetic diversity. The challenges of discontinuity in phenotype space, slow pace, and difficulty in covering the vast genetic space of multi-gene circuits hinder the use of Darwinian directed evolution for engineering advanced decision-making capabilities in living cells.

Here we report a new strategy for engineering complex multicellular gene circuits in living cells by developing a cellular adaptive sensor system, AdaptoCell, using modified *E. coli* cells. Our approach incorporates gene regulation into a synthetic plasmid heteroplasmy[28]

system that allows cells to maintain and adjust the expression of a red fluorescent protein and a specific resistance protein across generations. We engineer nine AdaptoCells, each sensing a different chemical. When grown together, they adjust their red fluorescence expression to match a specific nine-chemical pattern. We link the expression of the red fluorescent protein to a kanamycin resistance protein so that as the resistance protein increases, the red fluorescence decreases. This approach enables the use of sub-lethal kanamycin concentrations to permanently adapt the cells, resulting in lower expression levels of the red fluorescent protein. By choosing the AdaptoCells exhibiting the highest fluorescence, we can implement a decision-making process. This process involves exposing the cells to various chemical patterns, and if the decision produces an undesired outcome, we induce adaptation in the cells responsible for the incorrect decision. This iterative improvement method is repeated until the desired decision is achieved. We demonstrate this method by applying it to simple board games such as tic-tac-toe, a common benchmark in artificial intelligence[29]. We show that AdaptoCells can evolve to a state where they never lose a game. In summary, we report the creation and evolution of multicellular sensor systems called AdaptoCells, which can recognize and make decisions based on chemical patterns, as demonstrated through the example of mastering board games using an iterative improvement method.

Results

Sensor cells with synthetic plasmid heteroplasmy

We have advanced the concept of synthetic plasmid heteroplasmy by incorporating a conditional mechanism based on an external inducer. Synthetic plasmid heteroplasmy, as initially proposed[28], enables the stable maintenance of two plasmids in a population of *E. coli* cells with the ability to modify their relative copy numbers through encoded genetic machinery. This system is based on engineering multi-copy plasmids that carry the same antibiotic resistance gene, analogous to heterozygotic mutations observed in multi-copy plasmids[30] or mitochondrial DNA[31].To maintain plasmid stability, both plasmids must have

the same replication rate and genetic load, as differences can result in the loss of one plasmid type. However, maintaining plasmid composition across generations can be challenging when both plasmids express different gene expression cassettes in a constitutive manner[28], which prevents self-dosage. To overcome this limitation, we have improved synthetic plasmid heteroplasmy by making it conditional on an external inducer. This allows gene expression from both plasmids to switch off during normal cell growth and activate only when desired, resulting in equal genetic loads during growth and enhanced plasmid stability. Additionally, this conditional mechanism facilitates adaptation to chemical environments by allowing cells to alter their plasmid content after sensing a specific chemical inducer.

To engineer our synthetic heteroplasmy, we utilized two multicopy plasmids, P1 and P2, in populations of *Escherichia coli* Marionette strains (Fig. 1a). Both plasmids carried the same ampicillin resistance gene (AmpR) and origin of replication, regulating the stability of the total plasmid copy number ($a+b$), but not the individual copy numbers of P1 and P2. To ensure the stability of the individual copy numbers of P1 (a) and P2 (b), we designed the plasmids to have the same length and genetic load. We referred to the relative frequency of P1 in the cell as "weight", which was calculated as $a/(a+b)$. This weight serves as a genotype, as it maintains stability and consistency across generations, enabling us to predict the transmission of population-level traits and characteristics from parent to offspring. The plasmids encode a promoter from the Marionette cassette, enabling us to sense chemicals by using inducible promoters without any significant cross-interference, to regulate the genetic cargo of the plasmid heteroplasmy.

To easily measure the weight, we incorporated mCherry into the cargoes of P1 and EGFP into P2, enabling us to determine the weight through the fluorescence ratio of the mCherry and EGFP proteins. Additionally, we equipped the plasmids P1 and P2 with the ability to activate the fluorescence proteins and specific antibiotic resistance proteins after sensing a

151 specific chemical inducer (Fig. 1a). Both plasmids encode the same inducible promoter,
152 which regulates an operon with the fluorescent proteins and the fusions of antibiotic
153 resistance proteins (KanR/CmR for kanamycin/chloramphenicol resistance) or their
154 respective non-functional "dead" forms (dKanR/dCmR). We determine the weights through
155 fluorescence on a plate reader, flow cytometry, DNA quantification with sequencing[32], or
156 qPCR. Our results confirm that the population's weight stays consistent for several days (see
157 Extended Data Figs. 1a-c, 3b-d and Supplementary Text), aligning with a prior report[28].
158
159

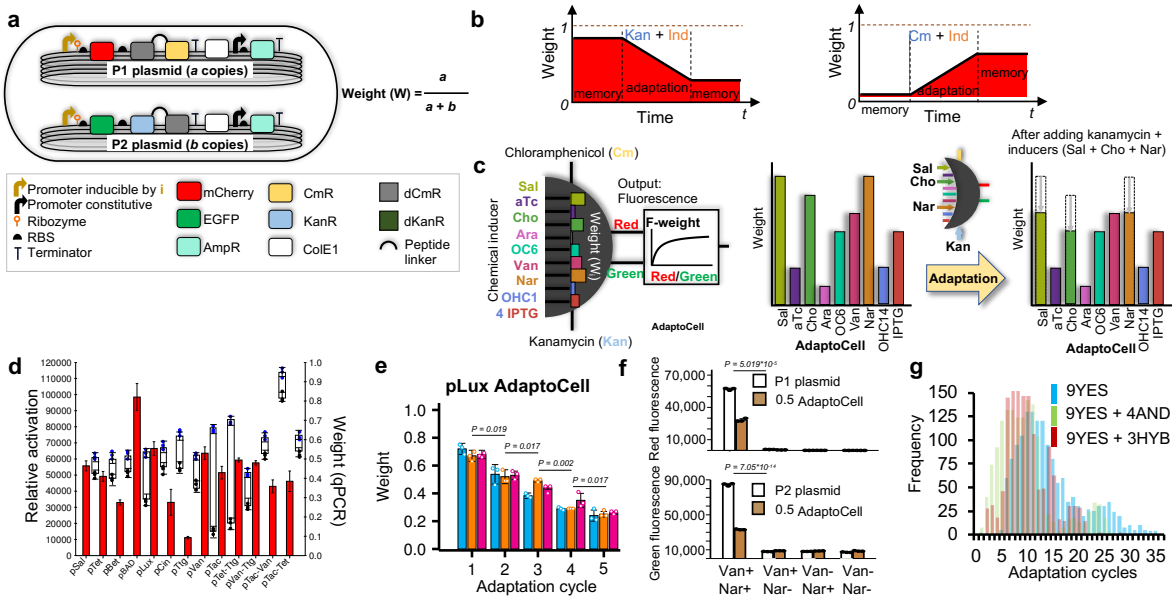

160 **Fig. 1 | Engineering stable genotypes in Escherichia coli through synthetic plasmid heteroplasmy. a**, We
161 combined two multicopy plasmids, P1 and P2, to create a synthetic plasmid heteroplasmy. P1 and P2 carry an
162 ampicillin resistance marker (AmpR) and a common replicon (ColE1) regulating the stability of the total copy
163 number (a+b), but not the individual copy numbers of P1 and P2 (a and b). In addition, the stability of a and b, is
164 maintained by designing the plasmids to produce equal genetic loads during replication preserving the relative
165 frequency of P1 in the cell, referred to as "weight". By incorporating mCherry into P1 and EGFP into P2, we can
166 determine the weight through the fluorescence ratio of the proteins when the promoters are fully active. To equip
167 the cells with the ability to detect chemicals, we integrated the same inducible Marionette promoter into both
168 plasmids. This promoter, triggered by the cognate chemical inducer "i," regulates the operon containing
169 fluorescent protein and antibiotic resistance protein fusions (KanR/CmR for kanamycin/chloramphenicol
170 resistance) or their non-functional counterparts (dKanR/dCmR). We implement a red fluorescence phenotype in
171 AdaptoCells through engineering a genetic link between the expression of a kanamycin resistance protein and a

red fluorescent protein. As the expression of the kanamycin protein increases, the red fluorescence decreases. **b**, The selection process using Kanamycin (Kan) or Chloramphenicol (Cm) amplifies the fraction of cells carrying the P2 or P1 plasmid (coding for KanR or CmR), which respectively reduces or increases the cell population's weight, but only when KanR or CmR are induced with a cognate chemical (ind). **c**, Antibiotic adaptation in AdaptoCells enables the simultaneous adjustment of multiple weights when adding the antibiotic in an environment representing a chemical pattern. For instance, the diagram illustrates the kanamycin adaptation of AdaptoCells when exposed to a chemical environment featuring high levels of Sal, Cho, and Nar inducers. The kanamycin adaptation only reduces the weight of the induced strains, leading to a lower red fluorescence output and F-weight when encountering again environments with the same Sal, Cho, and Nar levels. **d**, Characterisation in fluorescence and weight of the 9YES and 4AND AdaptoCell libraries containing 9 single-input and 4 dual-input promoters, respectively. Fluorescence variation upon induction (relative activation) of each AdaptoCell (red bars, left y-axis). Weight shown (right y-axis) before (blue) and after (black) one cycle of adaptation with kanamycin. **e**, Example of a 9YES AdaptoCell (pLux) of 0.6 weight, characterised after 5 consecutive adaptation cycles (see Extended Data Fig. 3 and 4 for the equivalent plots from flow cytometry, DNA sequencing and qPCR, for all the AdaptoCells). **f,** Normalised red and green fluorescence of one member of the 4AND AdaptoCell library (constructed by re-engineering the pVan promoter with the TtgR operator; see Methods and Extended Data Fig. 2b for the 3 other 4AND re-engineered promoters), with 0.5 weight, in the presence and absence of Vanillic acid (Van) and Naringenin (Nar) inducers. **g**, Distribution of the kanamycin adaptation cycles required to achieve mastery (100% expertise) in 1,500 3x3 board games for the 9YES, 9YES + 4AND and 3HYB (containing 3 hybrid AdaptoCells, see Box 1) AdaptoCell libraries. (data show mean ± s.d. for n=3 independent biological replicates).

Sub-lethal antibiotic selection produces adaptation in plasmid heteroplasmy

We hypothesized that the introduction of sub-lethal antibiotic concentrations would result in a biased alteration of the distribution, as cells harboring a higher number of plasmids encoding an antibiotic resistance protein will become enriched (in conditions where the appropriate inducible promoter is also chemically induced to express the antibiotic resistance gene). For instance, the combination of kanamycin and the chemical inducer allowed us to select cells that had the highest number of P2 plasmids. This is because the P2 plasmids carry the gene that makes the cells resistant to kanamycin and this gene is controlled by an inducible promoter. As a result of the selection process, the average number of P2 plasmids increased while the average number of P1 plasmids decreased. However, the total number

203 of plasmids (P1 and P2 combined) in the cells remained constant. This shift towards cells
204 with fewer P1 plasmids caused a decrease in the average red fluorescence per cell. The P1
205 plasmid is responsible for producing the red fluorescence protein mCherry. The
206 simultaneous addition of both the chemical inducer and antibiotic triggers the cells to alter
207 their weight, which in turn changes their fluorescence and antibiotic sensitivity activities. By
208 having the P1 and P2 plasmids contain a different inducible antibiotic resistance gene, the
209 addition of an antibiotic shifts the plasmid ratio towards the plasmid with the appropriate
210 resistance gene. Cells with higher numbers of P1 plasmid copies exhibit higher levels of red
211 fluorescence when the promoter is induced, but they are also more sensitive to kanamycin.
212 This is because they possess an inactive kanamycin resistance gene (dKanR), while the
213 active kanamycin resistance gene (KanR) resides on the P2 plasmid. The presence of
214 kanamycin and the chemical inducer prompts these cells to decrease their population
215 averaged P1 copy number, leading to a reduction in red fluorescence levels. The total red
216 fluorescence of AdaptoCells reflects the weighted average fluorescence among induced
217 strains. When kanamycin is added to an environment containing several of the nine
218 chemical inducers, it lowers the weights of the induced strains, causing a decrease in total
219 red fluorescence in that environment, but not in others (Fig. 1c). Thus, the total red
220 fluorescence can be modulated among different environments by trial-and-error only through
221 kanamycin adaptation, which lowers the red fluorescence in the targeted environments.
222
223 An AdaptoCell constitutes in fact a minimal gene circuit able to adapt its gene expression
224 when it is active, analogous to the memristor element used in electronic circuits with neural
225 network behaviour[33]. The promoter and KanR act as the computational and adaptation
226 engines respectively, where the promoter could be replaced by a more complex genetic
227 logic gate (Fig. 1d) (see Box 1 for generalisations).
228
229 **AdaptoCells libraries allow for the adaptation to chemical patterns**

230 We chose 9 different Marionette promoters to regulate the AdaptoCell's fluorescent proteins,
231 thus creating a base AdaptoCell library of 9 single-input AdaptoCells (9YES library,
232 characterised in Fig. 1d). We also extended the base library by re-engineering 4 Marionette
233 single-input promoters to have an additional input. These conditionally transcribe when two
234 specific chemicals are present in appropriate concentrations, implementing an AND logic
235 gate. We call this library 4AND (see Fig. 1d,f and Extended Data Fig. 2b for their
236 characterisation). After induction with the cognate chemical(s), all the 9YES and 4AND
237 AdaptoCells showed a significant activation versus non-induced (or partially induced) states
238 (Fig. 1d, average ANOSIM of R=0.82, see Suppl. Table S5). To experimentally test a
239 generalisation of AdaptoCells (Box 1) for constructing other adaptive gene circuits, we built a
240 hybrid AdaptoCell (pBAD:pSal) whose P1 and P2 plasmids encode for the AraC-mediated
241 activation and LysR-mediated repression of the pBAD and pSal promoters respectively. Its
242 functionality interpolates between a YES gate (0 and 1 weights) and an OR logic gate of the
243 promoters. We also constructed pTet:pBAD and pTet:pVan, creating the 3HYB library
244 (Extended Data Fig. 2c).
245
246 To analyse the capability of our libraries to successively adapt throughout several cycles
247 under the cognate inducer, we exposed our 9YES and 4AND libraries to consecutive cycles
248 of adaptation (Extended Data Fig. 3a). Each adaptation cycle involved overnight growth from
249 frozen stock, growth in presence of kanamycin and the respective inducers, and finally the
250 creation of another glycerol stock. After each cycle, the weights decreased significantly
251 ($p<0.05$), indicating adaptation. This was further validated by analysing the single-cell weight
252 distributions using flow cytometry (Extended Data Fig. 5a), where we inferred the weight
253 from a ratiometric analysis of the green and red fluorescence values (Methods and
254 Supplementary Text). The mean values of the distributions quantitatively agree with the
255 results obtained through plate reader fluorescence assay (average R^2 0.91, Extended Data
256 Fig. 4c). Our weight values after adaptation correlated with a model prediction of the effect of
257 adaptation on the single-cell weight distributions (R^2 0.92, Extended Data Fig. 5b). The

258 model only assumed that the antibiotic killed the cells having a red fluorescence higher than
259 a given threshold (Supplementary Text).
260
261 Now that we had libraries able undergo several rounds of adaptation, we asked to which
262 extent we could predict mCherry expression from an AdaptoCell's weight. We found that the
263 red fluorescence for 50 AdaptoCells of different weights from the 9YES and 4AND systems,
264 correlated well with weight obtained from DNA quantification (R^2 0.93, Extended Data Fig.
265 3a). We therefore developed a computational platform to simulate the decisions made by our
266 AdaptoCell libraries when subjected to successive adaptation steps. This allowed us to
267 examine if we could use our 9YES AdaptoCell libraries to construct a library of cells able to
268 learn any game played on a 3x3 board in a few adaptations. Given a set of weights,
269 expertise is defined as the percentage of positive results (wins and draws) assessed
270 computationally against all possible games. When we used a 9YES library for each position
271 (all AdaptoCells having equal weights, which implements a player with complete random
272 decisions) to play 1,500 different 3x3 board games, with kanamycin adaptation, we got
273 mastery (100% expertise) in less than 33 adaptations and often in a handful of adaptations
274 (Fig. 1g, Extended Data Fig. 10a,b, and Supplementary Text). Interestingly, when we
275 combined the 9YES and 4AND libraries, we reduced the mean of the adaptation rounds
276 required to achieve expertise from 11 to 6 and the maximum from 33 to 25. When we
277 combined the 9YES and 3HYB libraries, we reduced the mean of adaptation rounds from 11
278 to 8 and the maximum from 33 to 27 (Fig. 1g). Hybrid AdaptoCells also allow increasing the
279 computation capabilities without relying on the difficult engineering of combinatorial
280 promoters.
281
282
283
284
285

286

287 Box 1

288 Adaptive gene circuits

It is possible to generalise the concept of AdaptoCells to arbitrary gene circuits by replacing the genes chosen to modulate their expression levels with AdaptoCells. This requires at least as many compatible multiple-copy replicons than genes to modulate. Then, on each replicon we choose two genes under the same inducible regulation (transcriptional or post-transcriptional[34]). One gene should be the target gene for modulation and the other a selection gene. At least one of the copies of the replicon should encode a loss-of-function mutation (or a change in regulation) for the target and selection genes. For instance, panel **a** of the diagram below shows a cell with two transcriptional units encoded in two different compatible replicons[35], allowing for the adaptation of the genes *c* and *e* provided the genes *d* and *f* encode for a selection marker (or a CRISPR guide RNA targeting only the P1 copies of replicon 1). Note that the gene *e* doesn't need a loss-of-function mutation (denoted by crosses on the corresponding gene) because the P2 copies of replicon 2 have a different regulation. Panel **b** shows the adaptation of a metabolic pathway when the final product is able to induce the activation[36] of a gene c encoding a selection marker.

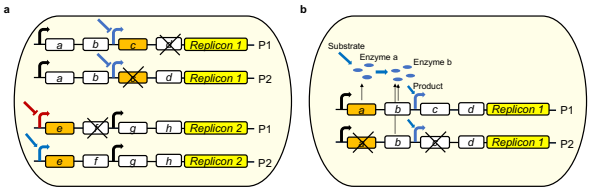

Examples of the implementation of AdaptoCells in gene circuits are:

Multi-gene adaptation
Rather than distributing sensor genes across independent AdaptoCells to adapt many genes simultaneously, as done in this study, we could co-transform more plasmids with compatible replicons (*e.g.* ColE1, p15A, CloDF13, ColA)[37] in a single cell using multiple heteroplasmy systems. We could design an AdaptoCell for each desired gene on each replicon, like genes *c* and e in diagram a, necessitating independent selection markers. For more than two intracellular AdaptoCells, a CRISPR selection marker might be advantageous[28]. It is also feasible to engineer adaptive gene circuits in eukaryotes by using multiple-copy DNA[38] and/or RNA[39] replicons.

Adaptation of gene circuit topology
It is possible to adapt the topology of a gene circuit by encoding promoters with different regulation on each of the AdaptoCell's plasmids, as shown in the diagram a with the promoter controlling gene *e*. In this example, it allows designing an adaptation that smoothly switches between a circuit where the promoter is activated to a circuit where the promoter is repressed. We show in Extended Data Fig. 2c an experimental validation.

Alternative selections
It is possible to use a negative selection marker (*e.g.* ePhe)[40] or to use a CRISPR/restriction system[28] against only one of the plasmids P1 or P2. If a loss-of-function mutation (*e.g.*, gene *c*) occurred on a gene conferring a cost/benefit to the cell, then selection (under inducing conditions) would decrease/increase the copy number ratio of the unmutated plasmid. Cell growth is not even strictly required for adaptation through selection because it is possible to use other mechanisms to change the total number of gene copies (*e.g.*, modulation of a replicon copy-number).

Multilayer adaptive gene circuits through AdaptoCell communication
AdaptoCells at different cells could be coupled through communication mechanisms (*e.g.*, quorum sensing[13]), creating a neural-like circuit. The reporter could also be a secreted chemical compound, where its inter-cellular accumulation would induce other cells with AdaptoCells.

Adaptive gene circuits in nature
We do not even require multiple-copy replicons if we have a multicellular population able to switch from growth and non-growth phases, such as stationary state bacteria or some tissues. In this case, a selection gene could pick a mutation in only a subpopulation of cells, which could be enriched through selection in the growth phase. Accordingly, it may be possible to infer AdaptoCells in natural microbial ecosystems[41] by identifying in such systems the mapping of environmental conditions, genes, inducible promoters, and selection markers with their mutations. This mapping would establish in fact a language for "teach the cells" algorithms. This may be relevant for applications in human health because multi-drug resistant plasmids[42], microbial or eukaryotic[43] consortia may already be using this type of adaptation to learn from the environment.

Fig. 2 | Box 1.

Antibiotic adaptation to change AdaptoCells decisions

By using multiple AdaptoCells, we can create a decision-making system. We define a decision among N categories by choosing the AdaptoCell with the highest red fluorescence among N independent AdaptoCells populations. For instance, in a 3x3 board game, we select the highest F-weight from the AdaptoCell populations at each available board position (Fig. 3a). To optimize the behavior of this system, we have designed an iterative improvement method. For example, when deciding among patterns of occupied board positions, we start by growing an initial set of N AdaptoCells independently. We then interrogate the system's decision by growing the N AdaptoCells in presence of the equivalent chemical pattern, either with saturating or vanishing levels of chemicals (Fig. 3b, where N=8). If the decision is not the desired one, we perform a kanamycin adaptation only to the AdaptoCells responsible for the decision (i.e., producing the highest red fluorescence). This process generates a new set of N AdaptoCells with updated AdaptoCells that underwent adaptation. We continue this process of adaptation until the decision changes.

The adaptation always lowers the red fluorescence, and since we consider the highest red fluorescence to decide, the decision will eventually change.

By strategically targeting the kanamycin adaptation to only the population with the highest F-weight, we cause a change in the decision, as the chosen culture's F-weight decreases and is no longer the highest. When a decision is not right in a given environment, we perform kanamycin adaptation with the AdaptoCells that have the highest F-weight in that environment, allowing us to gradually avoid poor decisions. When co-culturing heteroplasmy cells with several chemical inducers, the sub-lethal kanamycin selection will particularly affect cells with the highest red fluorescence. These cells' ability to adapt by lowering their fluorescence can impact decisions made based on highest fluorescence levels. To showcase the power of this strategy, we can use it in board games where there are no more than nine options per round. We map chemical inducers to the opponent's moves to determine the bacteria's decision (Fig. 3b). Multiple AdaptoCells co-cultures can serve as the bacterial player, playing against a trainer. The trainer makes selected moves, creating chemical patterns that induce the strains in the AdaptoCells populations, leading to the bacteria responding with their F-weights, with the highest weight signaling the next bacterial move. After a loss, we apply kanamycin adaptation to every AdaptoCell involved in the decision, considering the environment produced by the trainer's positions in each round. Over multiple lost matches, the AdaptoCells' weights decrease, avoiding repeating losing moves. This results in the bacteria never losing a match, regardless of the opponent's plays.

AdaptoCells adapt to play the tic-tac-toe game

We have chosen the common tic-tac-toe game to demonstrate a complex board game. The goal of the game is for either player to be the first to line up three of their symbol "X" or "O" in a row, column, or diagonal on the 3x3 board. Previous studies approached this game with DNA computing and 23 custom 3-input logic gates[21, 44], but these works did not involve living cells nor the capability to learn gameplaying. In our study, we assigned the first player as the

trainer (player X) and player O as a bacterial player, consisting of a set of AdaptoCells for each of the board positions (excluding the center, which is played first by player X). We assigned a chemical inducer to identify each of the 9 board positions of player X (center Fig. 3c). The cells play a match by measuring their F-weights through red and green fluorescence measurements (Methods and Supplementary Text). To determine O's move, we induce all co-cultures at unoccupied positions with the inducers assigned to X's played positions (experimental workflow in Fig. 4c, Methods and Supplementary Text). The co-culture with the highest F-weight decides O's next move. If O loses the match, we apply a kanamycin adaptation operation to the AdaptoCells only at the positions occupied by O (Fig. 3b). The next matches are played with the updated co-cultures.

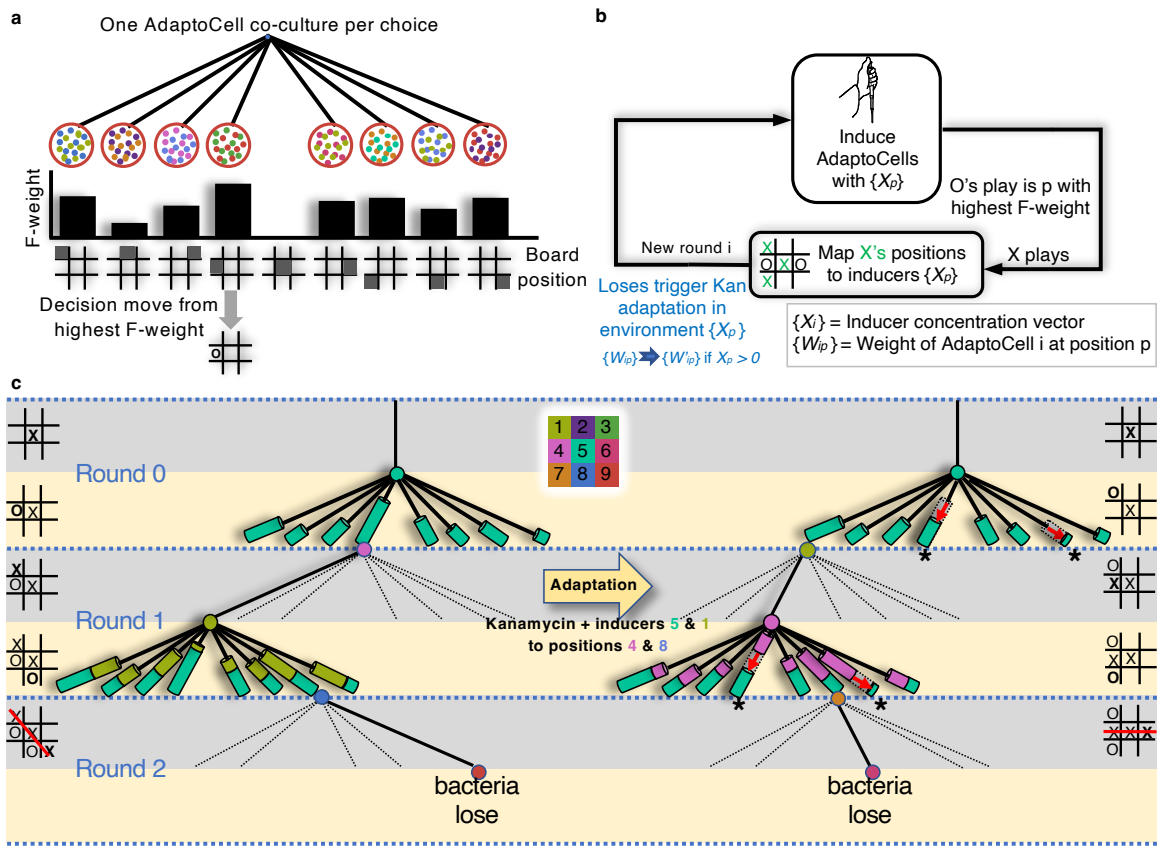

Fig. 3 | Decisions in tic-tac-toe game from chemical Induction and adaptation. a, The outcome of each round in a tic-tac-toe game is determined by incubating the AdaptoCells co-cultures with the inducers associated with the X player's moves, and measuring the highest F-weight to choose the bacteria's move. **b**, Diagram showing the iterative adaptation process that begins with growing the AdaptoCells in an environment defined by

the inducers mapped to the opponent's moves. The environment changes with each round as the opponent makes their move, which makes the cells respond differently. Only when player O loses, we perform a kanamycin adaptation in presence of the environment created during the losing match, which changes the state of the cells from O_i to O_{i+1}. **c**, Decision tree for the tic-tac-toe game shown as branches with cylinders of varying height to represent the weights for each strain of bacteria associated with a specific inducer, which represents the X player's move. In round 0, the branches show the weights for strain 5, which corresponds to inducer 5 (X player's position), at all possible positions. After inducing the co-cultures with chemical 5, the highest F-weight is the branch with the tallest cylinder height, representing the move of the bacterial player O. The X player then choses to move to position 1. In the following round, the cocultures at unoccupied positions are induced with all the inducers corresponding to X's positions, which in this case are chemicals 5 and 1. This creates an environment with inducers 5 and 1, so the weights for strains 5 and 1 are represented as stacked cylinders in the branches associated with all unoccupied positions for the bacterial player O. The game ends in the next round when X plays 9 and wins. Afterwards, a kanamycin selection operation is applied to only the cocultures at the positions played by player O (positions 4 and 8) in the presence of the inducers of X's moves from all rounds before the win (inducers 5 and 1). The X player's last move is not considered in this process because it did not create an environment to grow the AdaptoCells bacteria.

To measure the overall skill level of the game, similar to the Elo ranking[45], we run computer simulations of all possible games using the measured F-weights. These simulations, parametrized with our experimental data (Supplementary Text section 3.1, Table S2), evaluate the percentage of wins or draws (referred to as expertise) in all possible matches.

An illustration of a tic-tac-toe match is shown in Figure 3c. Player X starts at the center (Round 0) and player O can move to any of the 8 remaining positions. The F-weights of the co-cultures at those positions are measured by inducing them with the inducers assigned to X's move (3-oxohexanoyl-homoserine lactone, OC6, inducer assigned to 5, the center position). The position with the highest F-weight is selected as O's move. In the next round, X makes another move and O's move is determined by measuring the F-weights of the co-cultures at unoccupied positions after inducing them with both X's moves. O loses in Round 2, and a kanamycin adaptation operation is applied to the AdaptoCell populations at positions occupied by O. This adaptation updates AdaptoCell populations at positions 4 and

8. The bacteria continue playing matches until a match ends in a draw and player O demonstrates mastery.

AdaptoCells playing and adaptation Tic-Tac-Toe against one another

Players have AdaptoCell libraries of specific weights in cell cultures assigned to board positions (Fig. 4a), implementing the decision tree in Fig. 4e. We initially choose all cultures to have similar AdaptoCell weights (Fig. 4a). We performed a series of matches between the bacterial cultures (experimental workflow in Fig. 3c, Methods and Supplementary Text). To simplify the decision tree, at each round we allowed a maximum of 3 available positions (marked with blue dots) for each player (Fig. 4d).

After an opponent's move, we induce all permissible positions with the associated chemical input. The position with the highest F-weight is deemed the AdaptoCell's choice (Fig. 3a bottom). If maximal fluorescence values are similar (within one standard deviation), we randomly select the position (Fig. 4d, blue bars), ensuring decision tree exploration. The same results come from a single biological replicate, where the highest value dictates the decision, incorporating inherent biological randomness.

Expertise was assessed after each adaptation iteration by running simulations for all possible matches using the weights of the library measured from plate-reader fluorescence (Fig. 3f). To assess the adaptation capability of our AdaptoCell libraries, we simulated the libraries under a cycle of 10,000 randomised adaptations (Fig. 1g, Supplementary Text). Our experimental kanamycin adaptation allowed Player 2 to achieve mastery in only one adaptation more than the minimal rate of 2 adaptations (Extended Data Fig. 10c).

a

Player 1 (X)

Pos	Ind	AdaptoCell	Initial weight
1	4	pBAD	0.33 ± 0.03
2	9	pTac	0.76 ± 0.04
3	4	pBAD	0.31 ± 0.04
3	6	pCin	0.41 ± 0.04
4	1	pSal	0.51 ± 0.05
6	3	pBet	0.62 ± 0.03
7	4	pBAD	0.36 ± 0.04
7	6	pCin	0.43 ± 0.04
8	3	pBet	0.62 ± 0.03

Player 2 (O)

Pos	Ind	AdaptoCell	Initial weight
1	5	pLux	0.95 ± 0.03
2	7	pTtg	0.72 ± 0.04
3	7	pTtg	0.71 ± 0.05
4	5	pLux	0.97 ± 0.01
6	1	pSal	0.53 ± 0.05
6	4	pBAD	0.66 ± 0.05
7	3	pBetI	0.80 ± 0.03
8	2	pTet	0.72 ± 0.03
9	1	pSal	0.57 ± 0.04

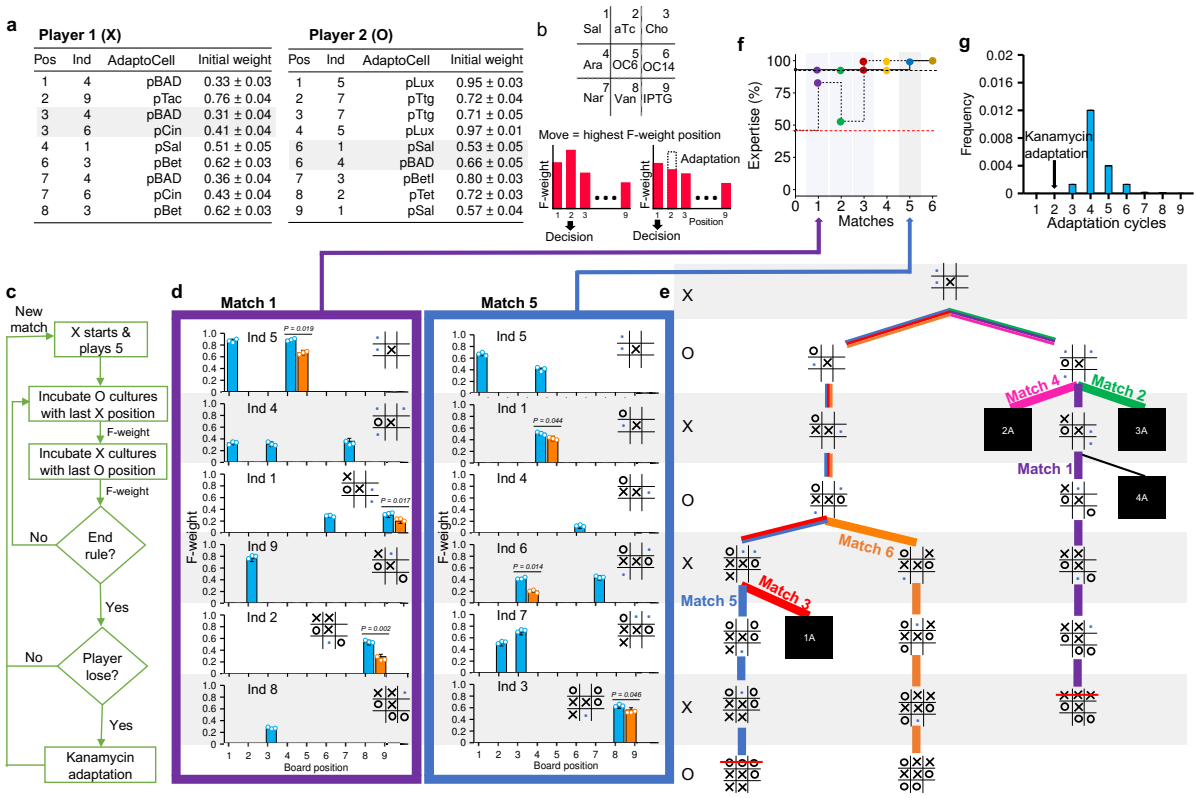

Fig. 4 | Two bacterial libraries undergo adaptation to master Tic-Tac-Toe by playing against one another. **a**. Libraries of AdaptoCell *E. coli* cultures designed to implement a restricted decision tree. We show the board position (Pos) and the number of the chemical (Ind) activating the AdaptoCell's promoter. The last column shows the weights measured by DNA sequencing before adaptation. Positions 3 and 7 for Player 1 and position 6 for Player 2 are assigned multi-cellular co-cultures of two AdaptoCells (Methods). **b,** Chemical inducers are mapped to board positions. **c**, Experimental workflow used in the matches. **d**, Two matches where kanamycin adaptation occurs, showing the board state before making a move. F-weights from AdaptoCell cultures before (blue) and after (orange) kanamycin adaptation (± s.d. for n = 3). Game board insets indicate the last move of the opponent and the permissible positions (blue dots) for the current move, restricted to limit possibilities. We do not allow for all unoccupied positions to restrict the number of possibilities, so we chose a few permissible positions. The position with highest F-weight gives the current move (shown aligned in panel **e**). **e**. The simplified tic-tac-toe decision tree, black boxes represent collapsed branches (Supplementary Text). Horizontal grey overlays align the decision tree to the decision taken by the bacteria in panel **d**. **f**, Expertise acquired during a tournament of 6 matches with both players suffering kanamycin adaptation. Filled circles denote the expertise (main text) after each game or after adaptation, colour-matching the frames in panel **d** (dotted line = player 2). Coloured overlays indicate the learner (grey = Player 1; blue = Player 2). Dashed lines indicate the expertise of non-learners (black = Player 1; red = Player 2). **g**, Histogram of the adaptation rounds required to achieve mastery in a computer simulation of 10,000 random tournaments, where for adaptation we used randomised inducers and kanamycin.

AdaptoCells can master arbitrary 3x3 board games

Next, we asked if our AdaptoCell libraries would be general enough to accommodate other well-known games such as chess, where pieces can be captured. A very simple variant is Hexapawn[46], which is played on a 3 x 3 board, with three chess pawns on each side. To further simplify the decision tree, we added the rule where pawns must capture if possible (Fig. 5b). We therefore designed custom AdaptoCell libraries for each bacterial player (Fig. 5a), implementing the decision tree in Fig. 5d. We ran a tournament until Player 1 reached mastery (Fig. 5c, Supplementary Text). The expertise increased after each adaptation iteration (Fig. 5f). Our experimental kanamycin adaptation only requires one extra adaptation over the best strategy (which we validated in a simulation of 10,000 randomised adaptations, Supplementary Text).

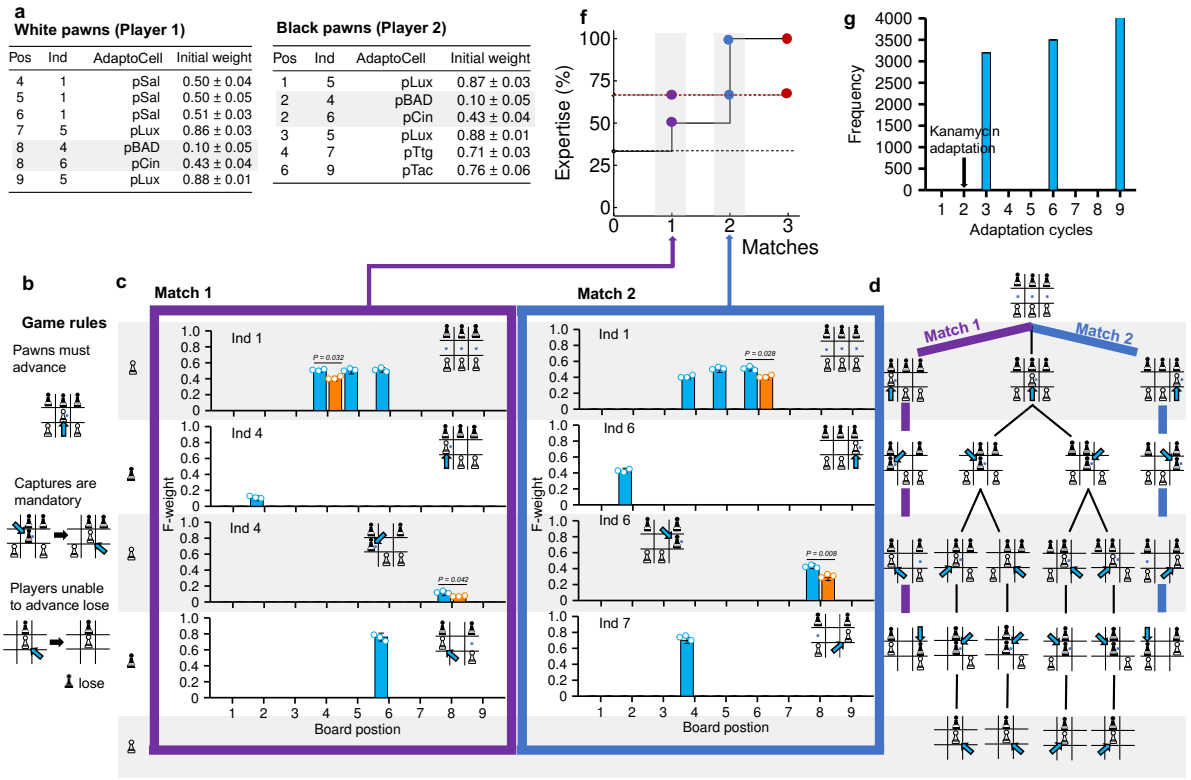

Fig. 5 | Two bacterial libraries playing and adaptation a simplified chess game in a 3x3 board (hexapawn). **a,** Libraries of AdaptoCell *E. coli* cultures chosen for the decision tree. F-weights were measured before

adaptation. Position 8 for Player 1 and position 2 for Player 2 are assigned co-cultures of two AdaptoCells (Methods). **b,** Rules of the game. **c**, Losses of the white pawns lead to kanamycin adaptation with kanamycin (F-weight before (blue) and after (orange) kanamycin adaptation (± s.d. for n = 3)). **d,** Decision tree for the AdaptoCell libraries. Blue dots indicate the available/mandatory moves. **e,** Expertise acquired during the tournaments with kanamycin adaptation after losing a game, (dotted line = player 2). Grey overlays indicate the adaptations of Player 1. Dashed lines indicate the expertise of non-learners (black = Player 1; red = Player 2). **f**, Distribution of adaptation rounds required to achieve mastery for a set of 10,000 simulations of tournaments where the adaptation used randomised inducers and kanamycin (similarly to Fig. 1g).

We now asked how much we could push our libraries to learn more complex game strategies experimentally. We considered a simplified variant of the game Go (also called Atari Go) in a 3x3 board, where the first capture ends the game[47]. We imposed a toroidal symmetry, where positions at the opposite sides of the board are considered adjacent (Extended Data Fig. 7, 8, 9) and we only allowed at each round a maximum of 3 available positions. A tournament with kanamycin adaptation for both bacterial libraries (Extended Data Fig. 7a) allowed reaching mastery in 5 adaptations (Extended Data Fig. 7b-c, Extended Data Figs. 8, 9). To further explore the limits of our 9YES library to learn new games, we used a naive 9YES library of 0.9 weights to achieve mastery, after successively playing adaptation tournaments of 3 and 20 cycles as first and second player of the full tic-tac-toe game, respectively (Extended Fig. 10d). Afterwards, the resulting library also achieved mastery at the toroidal Atari Go game after playing 1 and 6 adaptation cycles in the role of first and then second player (Extended Data Fig. 10e). Interestingly, the library was able to simultaneously master both games as first and second player (Extended Data Fig. 10f). When the resulting library was challenged to learn the most difficult game we sampled (we call 33L), it lost mastery at the previous two games (the second player expertise dropped to random levels, Extended Data Fig. 10g).

Our libraries reached mastery against non-expert players; playing against experts could accelerate adaptation through increased losses. We anticipate the weights could diminish for highly challenging games, as experienced when mastering 33L after the simultaneous mastery of tic-tac-toe and toroidal Atari Go. A solution could involve an operation on all AdaptoCells, called AdaptoCell fusion, which could conserve the expertise while boosting the small (non-vanishing) weights (Extended Data Fig. 10, Supplementary Text).

Discussion

In summary, we have developed a strategy to enable gene circuits to rapidly adapt to new behaviours by replacing designated genetic elements with AdaptoCells. AdaptoCells produce a gene expression that linearly correlates with their weights (Extended Data Fig. 4), which allows for the construction of gene circuits with predefined behaviour. For instance, using a AdaptoCell of weight 0.5 will be equivalent to using a traditional gene circuit with an engineered promoter with half of its transcription rate. Currently, the engineering of promoters of a targeted transcription rate requires screening mutant libraries[48, 49]. The AdaptoCells could be generalised in multicellular computing to arbitrary gene circuits by permitting the replacement of all genes in a decision circuit with AdaptoCells.

Our AdaptoCell system offers a unique solution to the limitations faced in traditional quantitative control over gene expression levels. Rather than offering direct control, our system allows for simultaneous relative adjustments to all the induced sensor strains' weights through the presence of chemical inducers and sub-lethal kanamycin. The weights of each sensor strain are linked to fluorescence, providing immediate feedback to the experimenter on the changes made. This enables a progressive adaptation towards a desired behavior without the need for prior knowledge of the optimal weights or manual weight setting.

128

129 Examining the capabilities of AdaptoCells as a single-layer artificial neural network (ANN)[50,
130 51] or perceptron reveals valuable insights. The tic-tac-toe AdaptoCell libraries associated to
131 each board position would correspond to a network of eight 9-input neurons and 72 synaptic
132 weights. As ANNs with positive weights and decisions based on the highest output signal
133 can approximate any function[52], we anticipate that the AdaptoCells could learn many games
134 on a 3x3 board. Unlike traditional backpropagation algorithms[53], our adaptation method does
135 not require knowledge of the weights or computation of the prediction error, making
136 AdaptoCell adaptation more closely mimic the functioning of the brain. This "training" is
137 achieved through repeated rounds of kanamycin adaptation, using chemical patterns and
138 red fluorescence protein expression levels as input and prediction output. Incorrect decisions
139 trigger a decrease in the weights of the responsible AdaptoCells, leading to gradual
140 improvement and optimized decision-making. In the same way that a perceptron can be
141 extended to multilayer ANNs, AdaptoCells can be extended to higher orders through cell-cell
142 communication, like other multicellular circuits[3, 4] (box I).

143

144 The improved adaptation in our extensions of the 9YES library to more complex promoter
145 regulations, combinatorial (4AND library) or hybrid (3HYB), suggests that by extending our
146 gene circuits (Box 1) to include more complex regulations would enhance the adaptation
147 capability. Moreover, the use of libraries of hybrid AdaptoCells together with the use of
148 appropriate selections (Box 1) provides a general way to adapt the topology of gene circuits[54]
149 (Extended Data Fig. 2). The 9YES library could also learn all the 1,500 games we tested, and
150 it could even simultaneously master more than one game (Extended Data Fig. 10), showing
151 that the information stored in the weights was still enough to learn new different algorithms.
152 This highlights the aptitude of 9YES for general-purpose adaptation. But, when pushing the

9YES library towards its limits, we found that it was not able to learn the 33L game without losing the mastery at toroidal Atari Go, suggesting that we possibly reached its adaptation capacity.

As the adaptation of gameplaying includes as a particular case the adaptation of the input patterns associated to a winning game, AdaptoCells may be used in applications such as pattern discrimination problems in therapeutics[55], where a reengineered microbiome is trained to adapt to certain chemical patterns, triggering a specific therapeutic delivery. AdaptoCells preserved their weight through growth cycles alternating with stationary states, both in liquid and solid cultures over several days (Extended Fig. 1, 3b,d), implying potential use in ecosystem-level gene circuits[56]. AdaptoCells could also be used with alternative selection markers, in single-cell circuits, or to explore alternative circuit topologies (Box 1). We could foresee adding an extra AdaptoCell library to each player that would receive the output of the first library through a cell-cell communication system (Box 1), mimicking a hidden layer in a neural network. This would enable the processing of more complex information and, therefore, adaptation more advanced games. Further developments could involve a way to genetically encode the computation of the maximum output among positions[17], as well as research into the possibility of naturally occurring AdaptoCells in prokaryotic or eukaryotic systems as a non-Darwinian adaptation tool[57] (Box 1). Kanamycin adaptation with AdaptoCells provides a strategy for the unsupervised adaptation of complex gene circuits with a large, unknown number of interactions, which will allow for the engineering of genetically-encoded general-purpose computational devices capable of self-adaptation.

176 **Material and methods.**

177 **Strains and growth media**. Cells were routinely grown aerobically at 37 °C in 14-ml tubes
178 (Supplier Scientific Laboratory Supplies Ltd, UK) in LB (1% tryptone, 0.5% yeast extract and
179 1% NaCl), LB agar plates (1.5% Select agar, Sigma Aldrich), or M9 medium (1x M9 salt
180 (Sigma Aldrich), 100 μM $CaCl_2$, 2 mM $MgSO_4$, 10 μM $FeSO_4$, glycerol 0.8% v/v) supplemented
181 with casamino acids 0.2% w/v, 1 μg/mL thiamine, 20 μg/mL uracil, 30 μg/mL leucine, using
182 NaOH to adjust the pH to 7.4. The base strain for all cloning experiments was *Escherichia coli*
183 strain Top10 (genotype [F-mcrAΔ(mrr-hsdRMS-mcrBC) Φ80lacZΔM15ΔlacX74 recA1 endA1
184 araΔ139 Δ (ara, leu)7697 galU galK λ-rpsL (StrR) nupG]), which was grown in LB medium at
185 37 °C and 200 rpm with antibiotics. The default antibiotic concentrations used are:
186 carbenicillin, 80 μg/mL; kanamycin 50 μg/mL; ampicillin, 100 μg/mL; chloramphenicol, 34
187 μg/mL. When recovering a culture from frozen glycerol stock, bacteria were inoculated into
188 2ml LB medium and grown overnight at 37 °C, 200 rpm with ampicillin (100 μg/ml). The
189 chloramphenicol resistance gene from the Marionette DH10B strain was cured (eliminated) by
190 electroporating 60 ng pE-FLP plasmid[58] into their competent cells and selecting on 50 μg/mL
191 ampicillin agar plate at 30 °C for one day. This cured strain was used for all AdaptoCell
192 adaptations and characterisations.

193

194 **Plasmid construction**. All the plasmids were generated Gibson assembly[59] by relying on
195 gene synthesis and PCR using Q5 master mix DNA Polymerase (New England Biolabs, USA)
196 with 40-bp homology domains. DNA was purchased from Integrated DNA Technologies
197 (USA). The plasmids P1 and P2 were designed to have the same size (4,774 bp in total) and
198 a common backbone consisting of: origin of replication (medium copy number pMB1),
199 ampicillin resistance cassette (from the pSEVA191 plasmid[60]) and the spy terminator[61] to
200 isolate the promoter. The replicon pMB1 (derivative of ColE1) was amplified from the plasmid

201 pWT018e (Addgene #107886)[28] by introducing a mutation in the RNAII gene (T to C) to lower
202 the copy number[62, 63]. To create the AdaptoCell libraries, a promoter-specific spacer followed
203 by the promoter were inserted into the common backbone plasmid of both P1 and P2 plasmids
204 (except for the hybrid AdaptoCell of Fig. 1i, where each plasmid has a different promoter). A
205 terminator was introduced when the plasmid size restriction allowed for it (Supplementary
206 Information). The promoter was followed by a promoter-specific spacer and by a RiboJ
207 ribozyme insulator[64] used to insulate the downstream transcript. The RiboJ was followed by a
208 weak ribosome-binding site (BBa_B0064 from the Registry of Parts) and by the mCherry (from
209 plasmid from PAJ310[65], with a C-terminus addition of a Gly-Ser-Gly amino acid sequence to
210 match the size of EGFP) and EGFP (from plasmid pWT018a) genes for the P1 and P2
211 plasmids respectively. After the fluorescent protein genes, the antibiotic resistance cassette
212 CmR-dKanR and dCmR-KanR from pWT018e and pWT018a was added polycistronically
213 (using the ribosome-binding site BBa_B0064) to the plasmids P1 and P2 respectively. CmR-
214 dKanR contains a chloramphenicol resistance gene fused (using a Gly-Ser- Gly-Ser- Gly-Ser
215 linker) to a kanamycin resistance gene with a Asp208Ala amino acid mutation to obliterate its
216 activity. dCmR-KanR contains a chloramphenicol resistance gene with a His195Ala amino
217 acid mutation to obliterate its activity (and an Ala29Thr amino acid mutation that appeared
218 during our cloning) fused to a kanamycin resistance gene using a Gly-Ser- Gly-Ser- Gly-Ser
219 linker.
220
221 **Combinatorial promoter engineering**. Our approach to engineering combinatorial
222 promoters involved integrating transcription factor operator sites into existing promoters,
223 aiming to trigger expression only when two specific chemical inducers reached sufficient
224 concentrations (AND logic gate on the inducers). This precisely tuned response was achieved
225 by incorporating operator sites from different transcription factors into various promoters from

226 the Marionette library at exact locations, while ensuring no interference with -10 and -35
227 sequences and those upstream of -35. Beginning with the pTac-Tet promoter, we incorporated
228 a 19 base pair (bp) tetO2 operator. The pTac-Van promoter was enhanced by the addition of
229 a 30 bp VanO2 operator, as described by Gitzinger et al. in 2012, differing from the operator
230 previously used in the Marionette study. Similarly, this modified VanO2 operator was also
231 introduced into the pTet-Van promoter. For the pTet-Bet promoter, we designed a novel 22 bp
232 BetO operator, inspired by the work of Stanton et al. 2013. The pTet-Ttg promoter was
233 modified by integrating a 30 bp TtgR operator from Krell et al. 2007, which deviates from the
234 operator in the Marionette paper by two bases. We inserted a 30 bp PhlF operator from Abbas
235 et al. 2002 into the pTet-PhlF promoter, placed in reverse orientation to avoid potential
236 interference with a -10 sequence. The pVan-Ttg and pVan-Tac promoters were equipped with
237 the TtgR operator from Krell et al. 2007 and the symmetric version of the lacOsym operator
238 from Lutz et al. 1997, respectively. Similarly, the symmetric lacOsym operator was included in
239 the pBet-Tac, pTtg-Tac, and pPhlF-Tac promoters. For the 4ANDMEM library, we engineered
240 the combinatorial promoters pTet-Ttg, pTac-Van, pVan-Ttg, and pTac-Tet by embedding
241 operators for TtgR[66], VanR[67], TtgR[66] and TetR[68] downstream of the pTet, pTac, pVanCC, and
242 pTac promoters[68] at positions +1, +20, +5, and +20, respectively. These operators spanned
243 lengths of 30 bp, 30 bp, 30 bp, and 19 bp. The TtgR operator was oriented in reverse to
244 prevent the formation of a tandem promoter, owing to its inherent -35 and partial -10
245 sequences.
246
247 **AdaptoCell transformation**. To create a cell carrying a AdaptoCell, the P1 and P2 plasmids
248 were co-transformed at equimolar concentrations (80 ng each) in the cured *E. coli* Marionette
249 DH10B strain. AdaptoCell selection was achieved on LB agar plates with ampicillin (60
250 µg/ML), kanamycin (17.5 µg/mL), chloramphenicol (11 µg/mL) and cognate chemical inducers

251 for the promoter(s) in the AdaptoCells. The concentrations for the chemical inducers (pSal:
252 Sal, Sodium salicylate; pTet: aTc, Anhydrotetracycline HCl; pBetI:Cho, Choline chloride;
253 pBAD: Ara, L-Arabinose; pLux: OC6, 3OC6-AHL; pCin: OC14, 3OHC14:1-AHL; pTtg: Nar,
254 Naringenin; pVan: Van, Vanillic acid; pTac: IPTG, Isopropyl-beta-D-thiogalactoside) are: pSal
255 (Sal 60 μM), pTet (aTc 0.1 μM), pBetI (Cho 6,000 μM), pBAD (Ara 2,000 μM), pLux (OC6 6
256 μM), pCin (OHC14 5 μM), pTtg (Nar 250 μM), pVan (Van 40 μM), pTac (IPTG 250 μM), pTet-
257 Ttg (aTc 0.1 μM, Nar 250 μM), pVan-Ttg (Van 25 μM, Nar 250 μM), pTac-pTet (IPTG 250 μM,
258 aTc 0.1 μM), pTac-Van (IPTG 250 μM, Van 25 μM). When P1 and P2 had different promoters
259 (Fig. 1i), they were both induced with their cognate chemicals. Single colonies were picked
260 and grown overnight with ampicillin (100 μg/ml). On the next day glycerol stocks were made
261 and stored them at -80 °C until use.
262
263 **AdaptoCell stability**. Glycerol stocks of bacteria carrying AdaptoCells were inoculated and
264 grown them overnight with ampicillin (100 μg/ml) in either liquid or solid LB medium. The
265 following day, a sample was taken from the culture to make glycerol stock and stored at -80
266 °C while the main culture continued to grow. We repeated this process for 5 days.
267
268 **AdaptoCell adaptation**. Glycerol stocks of bacteria carrying AdaptoCells were inoculated and
269 grown them overnight with ampicillin (100 μg/ml) after which the cultures were diluted 1:200
270 into freshly prepared 1.5mL M9 medium with carbenicillin, cognate inducer and custom
271 kanamycin concentrations for each AdaptoCell: pSal 1.5 μg/mL, pTet 2.5 μg/mL, pBet
272 4 μg/mL, pBAD 2.5 μg/mL, pLux 1 μg/mL, pCin 1.5 μg/mL, pTtg 1.5 μg/mL, pVan 3.5 μg/mL,
273 pTac 4 μg/mL, pTet-Ttg 1.5 μg/mL, pVan-Ttg 1.5 μg/mL, pTac-Tet 1.5 μg/mL, pTac-
274 Van 1.5 μg/mL. The chemical inducers concentrations used for each AdaptoCell are: pSal (Sal
275 100 μM), pTet (aTc 0.2 μM), pBetI (Cho 10,000 μM), pBAD (Ara 4,000 μM), pLux (OC6 10

276 μM), pCin (OH14 7 μM), pTtg (Nar 1,000 μM), pVan (Van 100 μM), pTac (IPTG 500 μM), pTet-
277 Ttg (aTc 0.2 μM, Nar 1,000 μM), pVan-Ttg (Van 100 μM, Nar 1,000 μM), pTac-pTet (IPTG
278 500 μM, aTc 200 μM), pTac-pVan (IPTG 500 μM, Van 100 μM). After refreshment the culture
279 was split into three individual cultures which were then carried separately in subsequent
280 experiments. The resulting culture tubes were incubated for 8 hours at 37 °C with shaking
281 (200 rpm). Finally, glycerol stocks were made and stored at -80 °C. This process was repeated
282 4 or 5 times for each AdaptoCell. For the AdaptoCell adaptation in distributed multi-cellular
283 co-cultures, glycerol stocks of bacteria with AdaptoCells were inoculated and grown
284 separately overnight with ampicillin (100 μg/ml). The following day, cultures of bacteria with
285 different mermegulons were mixed in equal volumes, then the resulting mixture was split in
286 two parts, one made into glycerol stock and stored at -80 °C and the other part was used for
287 adaptation. The culture for adaptation was diluted 1:200 in LB and grown for 8 hours in
288 presence of carbenicillin, with the cognate inducer(s) and the specific kanamycin
289 concentration.
290
291 **AdaptoCell fusion**. This operation merges two cultures of the same AdaptoCell but different
292 weight. If a AdaptoCell of weight 0.5 is added to all the members of a library, the weights will
293 increase if lower than 0.5. However, the expertise of the library (for any game) remains
294 unchanged. Two glycerol stocks of bacteria carrying the same AdaptoCell of different weights
295 were inoculated and grown overnight with ampicillin (100 μg/ml). The cultures were grown
296 independently and before characterisation 200 μL of each were mixed and 200 μL was used
297 to make glycerol stock and stored it at -80 °C.
298
299 **AdaptoCell characterisation using fluorescence plate reader**. Glycerol stocks of bacteria
300 carrying AdaptoCells were inoculated and grown overnight with ampicillin (100 μg/ml). The

301 overnight culture was refreshed by diluting 1:2000 in freshly prepared M9 medium with
302 cognate inducer(s) and carbenicillin (80 μg/mL). The concentrations for the promoter's
303 chemical inducers were: pSal (Sal 100 μM), pTet (aTc 0.2 μM), pBetI (Cho 10 mM), pBAD
304 (Ara 4 mM), pLux (OC6 10 μM), pCin (OH14 7μM), pTtg (Nar 1 mM), pVan (Van 100 μM),
305 pTac (IPTG 500 μM), pTet-Ttg (aTc 0.2 μM, Nar 280 μM), pVan-Ttg (Van 25 μm, Nar 280 μM),
306 pTac-Tet (IPTG 500 μM, aTc 200 μM), pTac-Van (IPTG 500 μM, Van 21 μM). Following an
307 additional 3 hours of growth, 200 μL samples of each culture were added to a 96-well plate
308 (Custom Corning Costar) with both technical and biological replicates. The plate was loaded
309 in an Infinite F500 microplate reader (Tecan) at 37 °C with shaking. OD600 was assayed with
310 an automatic repeating protocol of absorbance measurements (600 nm absorbance filter) and
311 fluorescence measurements (465/35 nm excitation filter—530/25 nm emission filter for EGFP
312 and 580/20nm excitation filter -635/35 nm filter for mCherry) were taken every 15 min during
313 18 hours of growth. The F-weight (W), which agrees with the weight for a monoculture, was
$W = \frac{1 - \gamma \frac{G}{R}}{1 - \lambda\beta + (\lambda - \gamma)\frac{G}{R}}$ $\lambda = \frac{R^{P1}}{G^{P2}}$, $\beta = \frac{G^{P1}}{R^{P1}}$, $\gamma = \frac{R^{P2}}{G^{P2}}$
314 estimated by using:
315 where and R and G are the red and green fluorescence values of an AdaptoCell culture or co-
316 culture. R^{P1} and R^{P2} are the red fluorescence value of fully induced P1- and P2-only cells and
317 G^{12} and G^{P2} are the green fluorescence value of fully induced P1- and P2-only cells. We
318 approximated γ = 0. The λ and β values were computed for each promoter and are included
319 in Table S19. For the fluorescence characterisation of distributed multi-cellular co-cultures,
320 only one AdaptoCell was induced at a time and the weight of the mixed culture was multiplied
321 by the number of component strains.
322
323 **Fluorescence plate reader data analysis**. Excel (Microsoft) with bespoke macros was used
324 for data analysis (Supplementary Information). In summary, OD600 values were synchronised

325 at OD600 = 0.2, where linear interpolation was used to infer fluorescence (F) and OD600
326 values at non-measured times. The growth rate was fitted against an exponential and poor fits
327 (r^2<0.9) were discarded. The fluorescence reported was computed as a constant slope for a
328 non-linear fitting of the F to the OD600. The weight was calculated by the non-linear fitting of
329 the whole dynamics of the red fluorescence of the strain of interest against the red
330 fluorescence of P1-only cells averaged among biological replicates.
331
332 **AdaptoCell characterisation using flow cytometry**. Glycerol stocks of bacteria carrying
333 AdaptoCells were inoculated and grown overnight with ampicillin (100 µg/mL). On the next
334 day the cultures were refreshed with 200 µl dilution in 2 mL LB with carbenicillin (80 µg/mL)
335 and cognate inducer, and later incubated for 4 hours at 37 °C with 200 rpm shaking. The
336 concentrations for the promoter's chemical inducers were the same used for the plate reader
337 assay. After 4 hours of growth, when the log phase was reached, the cultures were centrifuged
338 at 3000 rpm for 10 minutes at 4 °C. The pellets were resuspended in 2 mL PBS solution and
339 200 µL samples were loaded in 96 well plate. The plates containing cell cultures were
340 processed using a BD LSRFortessa High Throughput Sampler (HTS) with the following
341 settings: at a Sample Flow Rate of 1ul/second; Sample Volume 5 µl; Mixing Volume 50 µl;
342 Mixing Speed 200 µl/sec; Number of Mixes 5; Wash Volume 200 µl; BLR Enabled. A maximum
343 of 50,000 events were recorded for each sample.
344
345 **Flow cytometry data analysis**. The weights were calculated with the equation (see
346 Supplementary Information for its derivation) weight = $1/(1+\lambda(\mathrm{G}/\mathrm{R}-\beta))$, where $\lambda =$
347 $R_{P1}/G_{P2}, \beta = G_{P1}/R_{P1}$. R_{P1} and G_{P1} are the mean red and green fluorescence of P1-only cells.
348 We computed lambda and beta for each promoter separately. Weight values higher than 1 or
349 lower than 0 were removed. We calculated the weight using the red and green fluorescence

350 values of the strain of interest. To predict a AdaptoCell's weight after a given number of
351 adaptation iterations, the 2% of cells with the highest red fluorescence were recursively pruned
352 followed by re-normalising the area of the distribution (Extended Data Fig. 5b, Supplementary
353 Text).
354
355 **AdaptoCell characterisation using Sanger sequencing**. Glycerol stocks of bacteria
356 carrying AdaptoCells were inoculated and grown overnight with ampicillin (100 µg/ml). The
357 plasmid DNA (GeneJET, Thermofisher) was purified for Sanger sequencing. Minipreps from
358 single-strain bacterial colonies carrying AdaptoCells were sequenced with the CamR reverse
359 primer annealing to a common sequence of P1 and P2. For distributed multicellular co-
360 cultures, forward primers specific to only one of the promoter regions of the AdaptoCells found
361 in the miniprep were used. All primers are included in Supplementary Table 5. Minipreps of
362 the P1- and P2-only cells were also sequenced with the CamR primer. The mixed read
363 chromatogram traces (AB1 files) from the Sanger sequencing (GATC, Germany) were kept
364 for subsequent analysis.
365
366 **Sanger sequencing data analysis**. To compute the weight, the mixed reads' chromatogram
367 traces from the Sanger's AB1 files were analysed by aligning them against the traces of P1-
368 and P2-only cells using a custom algorithm (Supplementary Information) implemented in
369 Biopython[69] (a recently published method[70] did not give adequate results for AdaptoCells). In
370 summary, our algorithm firstly aligns the chromatogram traces by basecalling them and
371 performing a sequence alignment against EGFP-mCherry. Afterwards, it estimates the weight
372 from the average ratio of the mixed read's peaks against the P1- and P2-only cells' peaks at
373 EGFP-mCherry mismatch positions. The EGFP-mCherry match positions were used to
374 normalise the traces.

375

376 **AdaptoCell weight characterisation by qPCR**. Glycerol stocks of bacteria carrying
377 AdaptoCells were inoculated and grown overnight with ampicillin (100 µg/ml). Plasmid DNA
378 was extracted using GeneJET Plasmid Miniprep Kit (Thermo ScientificTM, UK K0503) and
379 quantified using the NanoDrop® ND-1000 UV-Vis Spectrophotometer. Quantitative real-time–
380 PCRs (qRT–PCR) analyses were performed on the StepOnePlus™ Real-Time PCR System
381 (Thermo ScientificTM) using the Fast SYBR-Green master mix (Thermo ScientificTM, UK
382 K0503) and following the manufacturer's instructions. The P1 plasmid was quantified using
383 the RG1083 and RG1084 primers specific for the mCherry coding sequence. The P2 plasmid
384 was quantified using the RG1087 and RG1088 primers specific for the EGFP coding
385 sequence. The RG1080 and RG1082 primers which anneal to a common sequence of P1 and
386 P2 construct backbone were used as endogenous control for the relative quantification of
387 P1/P2 plasmids. All primers are included in the Supplementary methods.

388

389 **AdaptoCell fluorescence characterization in solid medium**. We surrounded the cocultures
390 on the agar plate with aluminum foil masks and transferred them to a new LB agar plate using
391 a standard replica plating procedure. Both the original and replica plates were incubated at 37
392 °C for 1 hour, and the original plate was further incubated for 6 hours to restore the cocultures.
393 We added 0.5 µl of the necessary inducers to the cocultures on the replica plate, and let the
394 cells grow for 6 hours at 37 °C. After that, we stored them overnight at 4 °C. To image the
395 cocultures for fluorescence expression, we used a blue LED (470 nm) transilluminator with an
396 amber filter unit (580 nm).

397

398 **Experimental strategy for gameplaying with AdaptoCell libraries in liquid medium**.
399 Bacterial cultures carrying AdaptoCells are assigned to each board position for each bacterial

400 player according to a specific game and decision tree. For positions with more than one
401 AdaptoCell, the cultures are grown individually or together as an equal volume co-culture. To
402 encourage both bacterial players to take random decisions before any adaptation,
403 AdaptoCells of equal weights within one standard deviation in their biological replicates are
404 initially chosen. Player 1 makes the first move. For tic-tac-toe and toroidal Atari Go, Player 1
405 initially plays in position 5. Moves are determined by the highest normalised red fluorescence
406 in plate reader across unoccupied (and allowed, in case of games with simplified decision
407 trees) positions after growing from glycerol the AdaptoCell cultures and inducing them with
408 the chemicals assigned to the opponent's positions. When positions contain more than one
409 culture, all the normalised red fluorescence values of those cultures are added. If the highest
410 red fluorescence involves more than one position (within one standard deviation in the
411 biological replicates) then we choose randomly among these positions. This cycle is repeated
412 until one of the ending rules is matched. At the end of each game, we assessed if any of the
413 two players has lost, case in which kanamycin adaptation was applied to the loser. For this,
414 AdaptoCell adaptation was conducted for each move played by adding the chemicals of the
415 opponent's positions and kanamycin. The glycerol stocks were updated and the matches
416 continued until both players reached mastery.
417
418 **Experimental strategy for gameplaying with AdaptoCell libraries in solid medium**. The
419 game is initiated by growing the AdaptoCell cultures, then distributing them across all positions
420 of a game board-like agar plate except the center. This plate, referred to as the parental plate,
421 which is only measured by replica-plating. The game proceeds in rounds where inducer
422 assigned to the positions occupied by player X, is added to all positions. After replica-plating
423 the parental plate, a period of incubation and cooling, the cultures are imaged for fluorescence
424 expression. The brightness of fluorescence is quantified using the equation for the F-weight

425 (eq. 2.1 in Supplementary Text), and the F-weight culture is considered player O's move. This
426 process is repeated for each round until a winning condition, or end rule, is met (see details
427 of the protocol in the Supplementary Text). If the bacteria lose the game, they undergo an
428 adaptation process, where we do a replica plating of the parental plate, where the cocultures
429 are exposed to inducers that represented the player X's moves in the rounds of the match,
430 and kanamycin. This is performed in a given incubation period (see Supplementary Text).
431 Then, another plating procedure is performed to halt the adaptation process and to remove
432 the inducers and kanamycin. After an overnight storage, a new parental plate with the newly
433 adapted bacteria is ready for the next game. The glycerol stocks are made and updated and
434 the matches continued until both players reached mastery.
435
436 **Computer simulation of bacterial gameplaying**. A C++ code was written to simulate the
437 capability of bacteria carrying AdaptoCells to play and learn different games. The red
438 fluorescence of a AdaptoCell is modelled by multiplying its weight to the promoter's effective
439 transcription rate. The effective transcription rate is fitted from our experimental data
440 (supplementary Text). Mimicking the experimental gameplaying strategy, the move of a player
441 is computed from the available position with highest fluorescence after having induced the
442 AdaptoCell's promoters with the chemicals corresponding to the opponent positions. Before
443 the start of a tournament, both players are set as learners. If a player loses a game, kanamycin
444 adaptation is applied by decreasing the weights of the AdaptoCells at the positions played by
445 a pre-defined coefficient of 0.05. To evaluate the expertise of a given set of weights
446 (corresponding to a AdaptoCell library), a player that plays randomly (uniform probability)
447 among available positions was used. This player was used as a non-learner to calculate the
448 expertise of the learners after each kanamycin adaptation by playing 10,000 games and
449 checking the percentage of positive results. This computation of expertise was also used with

450 an experimental AdaptoCell library once we have measured the weights by fluorescence or
451 DNA quantifications. The successive adaptation tournaments of tic-tac-toe, toroidal Atari Go
452 and 33L (Extended Fig. 10d) where done by playing each resulting 9YES library against a
453 new 9YES library (with starting weights equal to 0.9) able to learn by kanamycin adaptation.
454 The tic-tac-toe tournament after achieving mastery at 33L included a AdaptoCell fusion
455 operation at match 9.
456
457 **Randomised game rules and adaptations.** For Fig. 1d, we considered a 1,500-sample of
458 all possible games where the pieces cannot be moved nor captured. We generated 10,000
459 games with 110 random zero-sum end-of-game rules, each specifying 3 or 4 occupied board
460 positions defining winning or losing the match. To generate the adaptation tournaments used
461 in Fig. 3g, Fig. 4g and Extended Fig. 8h, we uniformly selected at random either 3 (Hexapawn)
462 or 4 (tic-tac-toe and toroidal Atari Go) AdaptoCells from the library of a player to undergo
463 kanamycin adaptation. Examples are included in Extended Data Fig. 10c.
464
465 **Statistical analyses**. All measurements were taken from distinct samples and the
466 experiments were not randomised. All Pearson's r coefficients were determined by linear
467 regression analysis. Non-parametric ANOSIM tests done with the Vegan R package were
468 used to assess the hypotheses of statistically significant differences between two bacterial
469 cultures transformed with AdaptoCells. AdaptoCell stability (Fig.1b), relative activation (Fig.
470 1d,i), and the weight decrease produced by kanamycin adaptation (Fig. 3e) were tested.
471
472 **Reporting summary.** Further information on research design is available in the Nature
473 Research Reporting Summary linked to this paper.
474

475 **Data availability**

476 All relevant data are included as Source Data and are available from the corresponding author
477 on reasonable request. Strains and plasmids used in this study are available from the
478 corresponding author on reasonable request and from the Addgene repository.

479 **Code availability**

480 The software used for simulations and data analysis is available from the corresponding
481 author on reasonable request.

482

483 ## Acknowledgments

484 RG acknowledges the departmental allocation from the School of Life Sciences (Faculty of
485 Natural Sciences, Keele University). MI acknowledges funding from BBSRC BB/P020615/1
486 (EVO-ENGINE) and the Volkswagen Foundation (LIFE: 93 065). AJ was funded by the
487 Ministerio de Ciencia e Innovacion GeneCircuits++ PID2020-118436GB-I00
488 (GeneCircuits++), BBSRC BB/P020615/1 (EVO-ENGINE), EU grants EVOPROG 610730
489 and PhotoSynH2 HORIZON-EIC-2021-PATHFINDERCHALLENGES (grant agreement
490 101070948), EPSRC-BBSRC BB/M017982/1 (WISB centre), ONRG (BacMorse), and the
491 departmental allocation from the School of Life Sciences (U. Warwick). We thank J.
492 Penadés, M. Kushwaha and V. de Lorenzo for their comments.

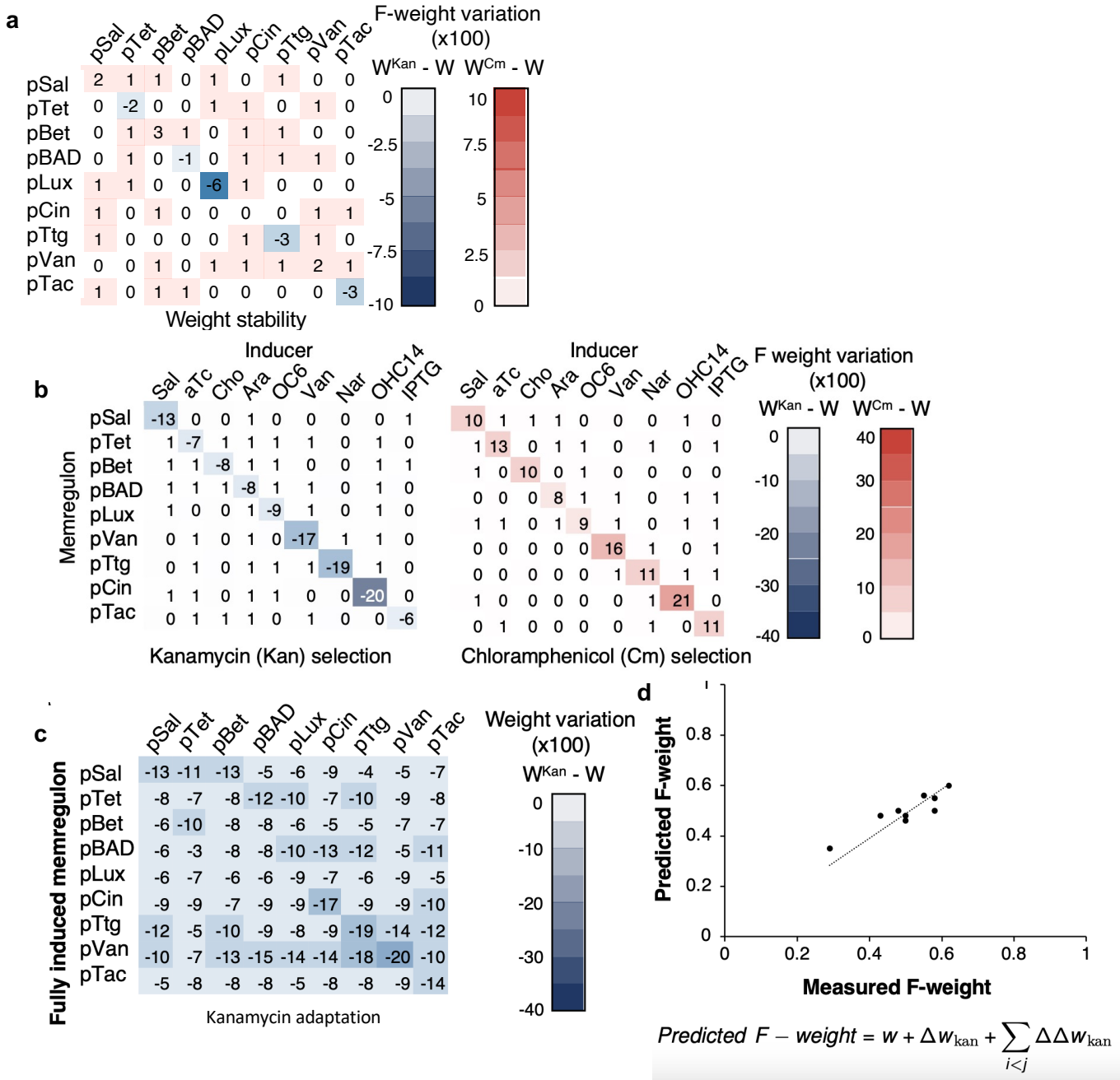

Extended Data Fig. 1 | F-weights are stable in AdaptoCell mono- and co-cultures. a, After four days of daily replica plating, freezing and replica copying, the F-weight variation in co-cultures of two AdaptoCell strains demonstrates minimal and non-statistically significant change (lowest p>0.1). This data informs a pairwise model (refer to Supplementary Text and panel **d**). **b**, Adaptation of single-sensor AdaptoCell strains is activation-dependent. Statistically significant weight variation (p<0.01) occurs when strains grow on agar plates with the orthogonal inducer, under kanamycin or chloramphenicol selection. The inducer and antibiotic concentrations are detailed in the Methods. **c**, Composition of co-culture influences kanamycin adaptation. Co-cultures of two memregulon strains exhibit significant fluorescent weight variation (p<0.05) under kanamycin adaptation when only one component strain is fully induced. Culturing two AdaptoCell strains together results in less weight variation during kanamycin adaptation, as inactive promoter cells' reduced growth artificially boosts the weight of active promoter cells. **d**, A pairwise model using the F-weight variation in co-cultures of two AdaptoCell strains (as done in panel **a**) can predict the F-weight variation in co-cultures of nine AdaptoCell strains (R2=0.91).

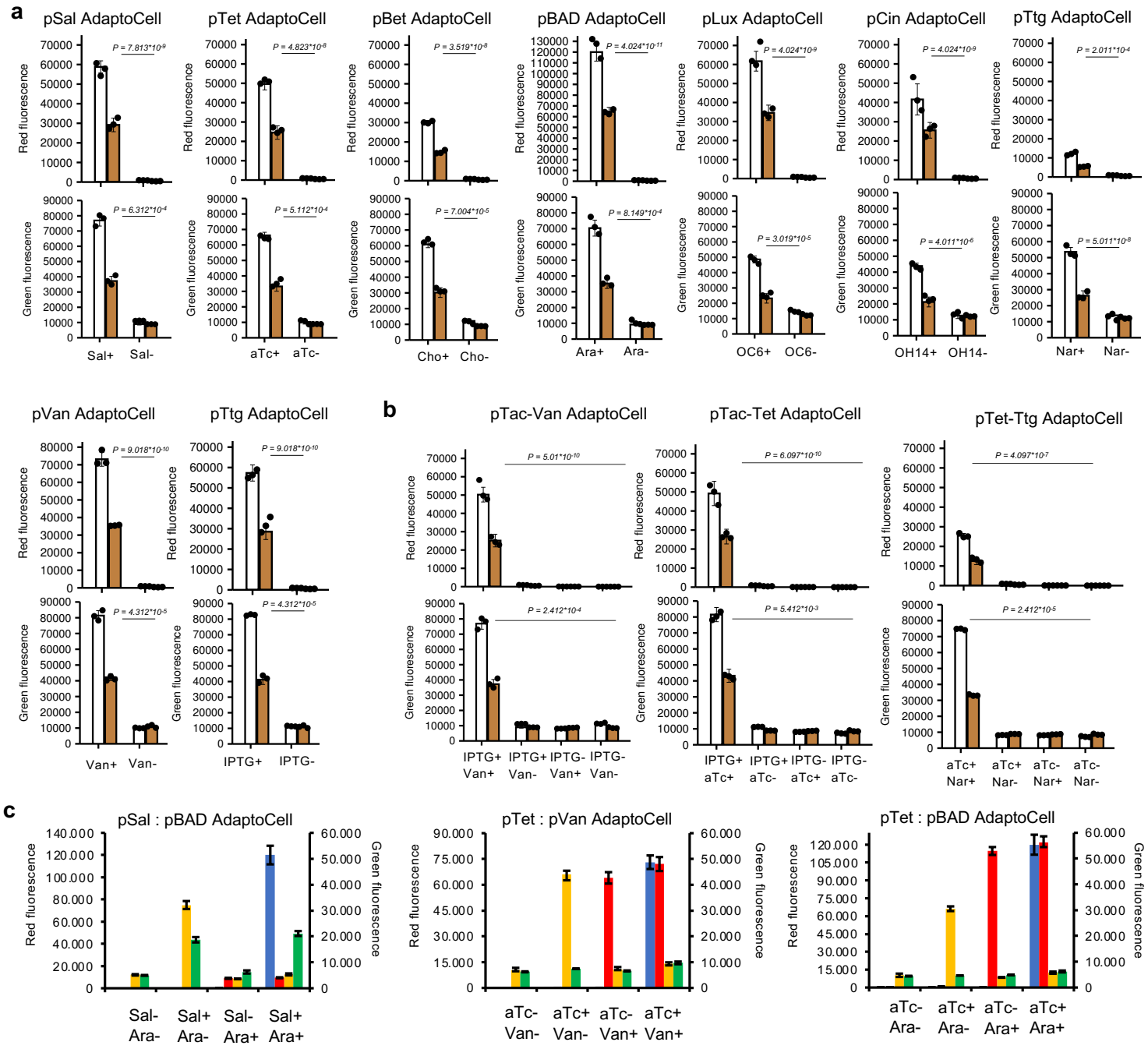

Extended Data Fig. 2. | AdaptoCell computation capabilities. Red and green fluorescence of cells transformed with either P1 or P2 (white-filled bars) and 0.5 weight AdaptoCells (brown bars) grown in presence (at saturating levels, see Methods) or absence of cognate inducer for the 9YES AdaptoCell library (**a**) the 3 remaining 4AND library members (see Fig. 1), (**b**), and the 3HYB library (**c**). The 4AND and 3HYB libraries are grown in the presence or absence of each of the two cognate inducers.

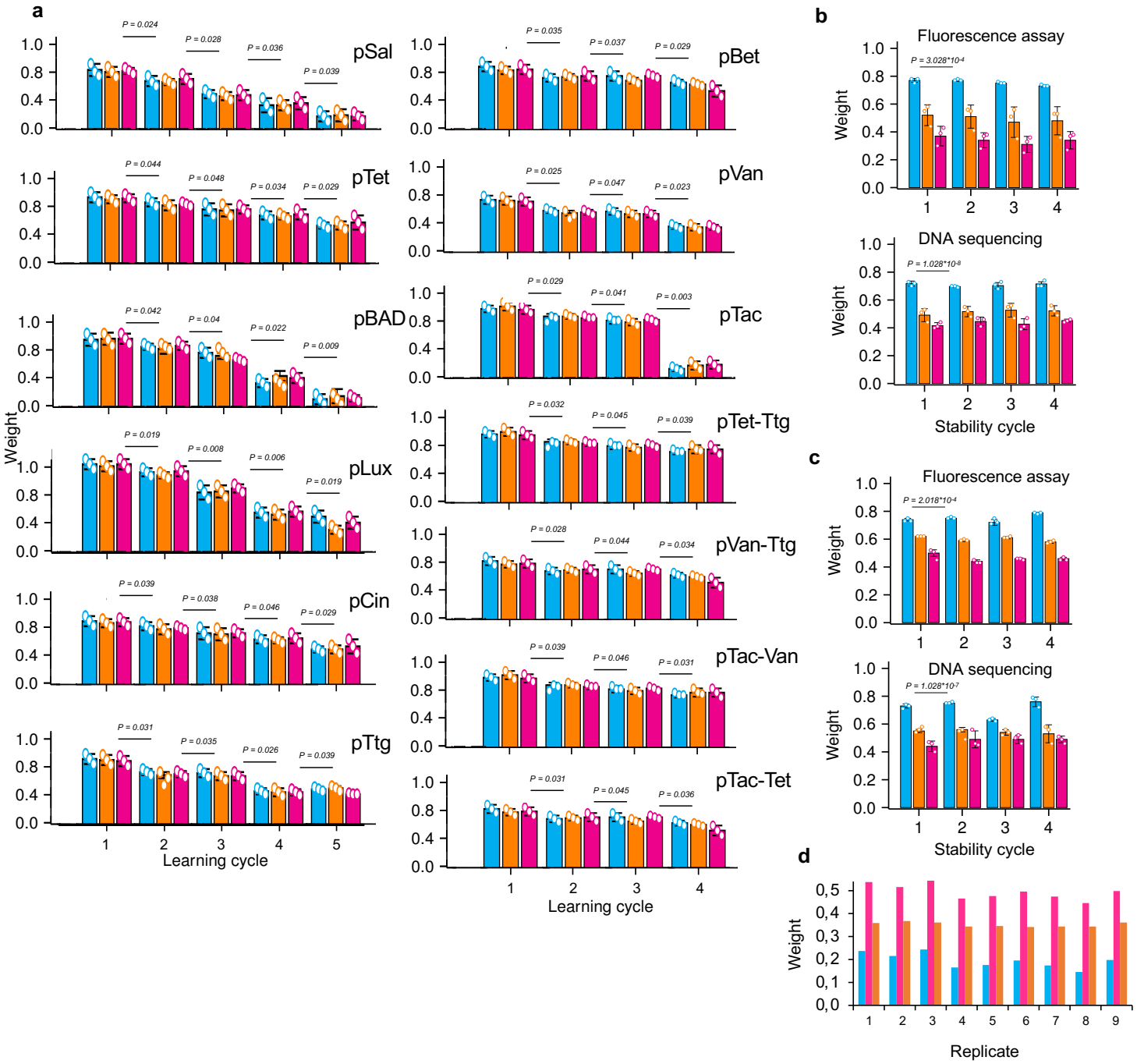

Extended Data Fig. 3. | Adaptation and stability of AdaptoCell's gene expression. a, Fluorescence analysis-based weights (F-weights) of 9YES and 4AND AdaptoCell libraries following five and four sequential adaptation experiments, respectively (for equivalent DNA sequencing plots, see Supplementary Information). Different colors denote different lineages. **b**, pBAD AdaptoCell weight, as measured through fluorescence plate reader assay and DNA sequencing, for three different AdaptoCells in stationary state liquid cultures at 37°C, without induction or adaptation. **c**, pBAD AdaptoCell weight in stationary state solid medium cultures at 37°C, absent induction or adaptation. **d**, Fusion operation characterization showing preservation of any player's library expertise for a given game. We added an equal volume of the same AdaptoCell culture (pBAD with a 0.5 weight) to a given AdaptoCell culture (pBAD). Weight measurements, via ratiometric fluorescence assay, before (blue bars) and after a 1:1 co-culture (orange bars) with a pBAD AdaptoCell of weight 0.5 (red bars) are shown. AdaptoCell fusion (refer to Supplementary Text) helps maintain weights after numerous kanamycin adaptations, facilitating continued adaptation.

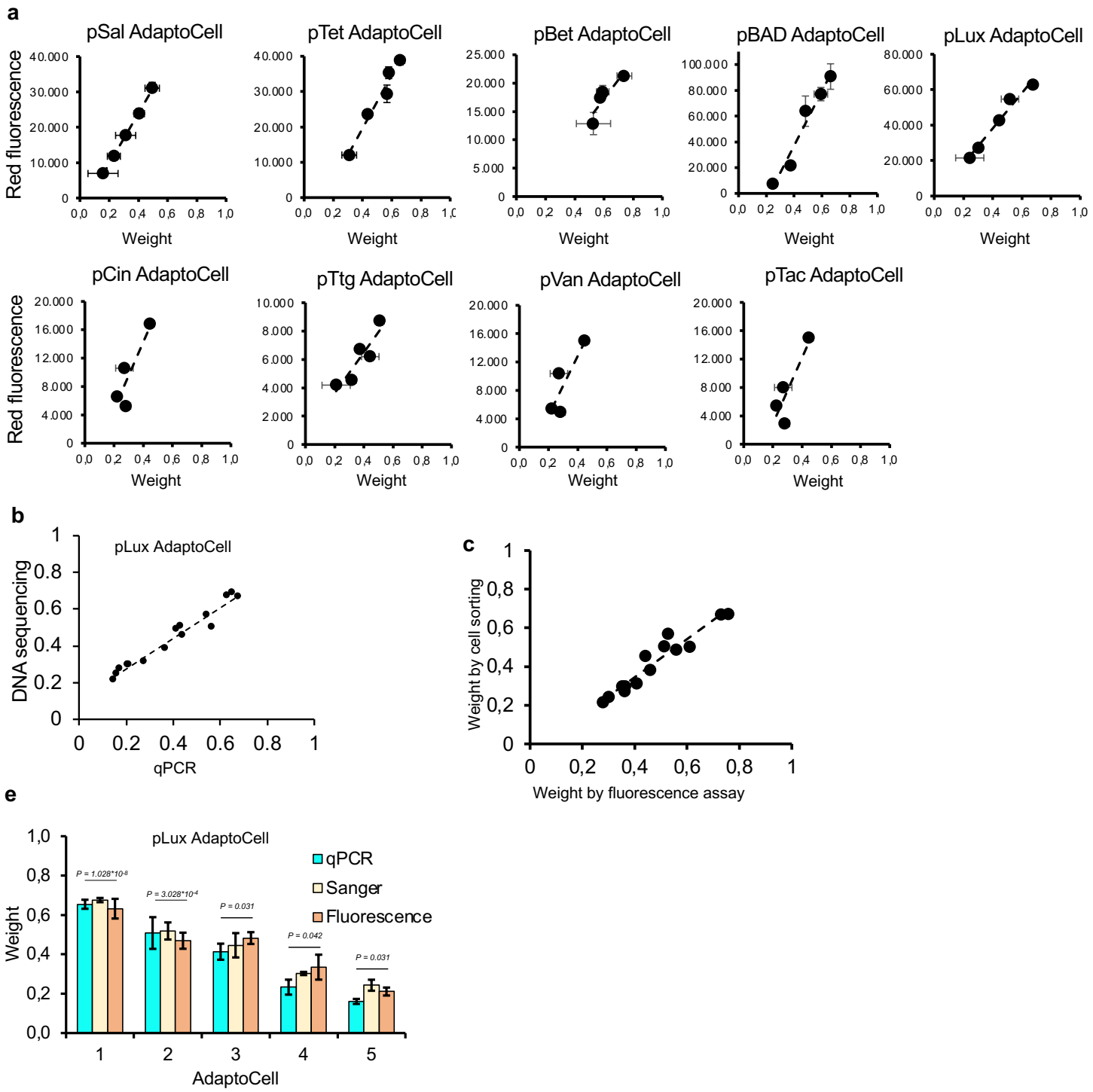

Extended Data Fig. 4. | AdaptoCell's weight measurement agree when using different techniques. a, AdaptoCells of different weights give a predictable gene expression (R^2=0.99, (± s.d. for n = 3). **b,** Correlation between weights measured by Sanger sequencing against qPCR data. **c**, Correlation between weights measured by cell sorting against fluorescence assay for the pLux AdaptoCell. (R^2=0.92) **e,** Example of simultaneous characterization of each round of adaptation of the pLux AdaptoCell using Sanger sequencing, qPCR and fluorescence assay data (averge ANOSIM R=0.82).

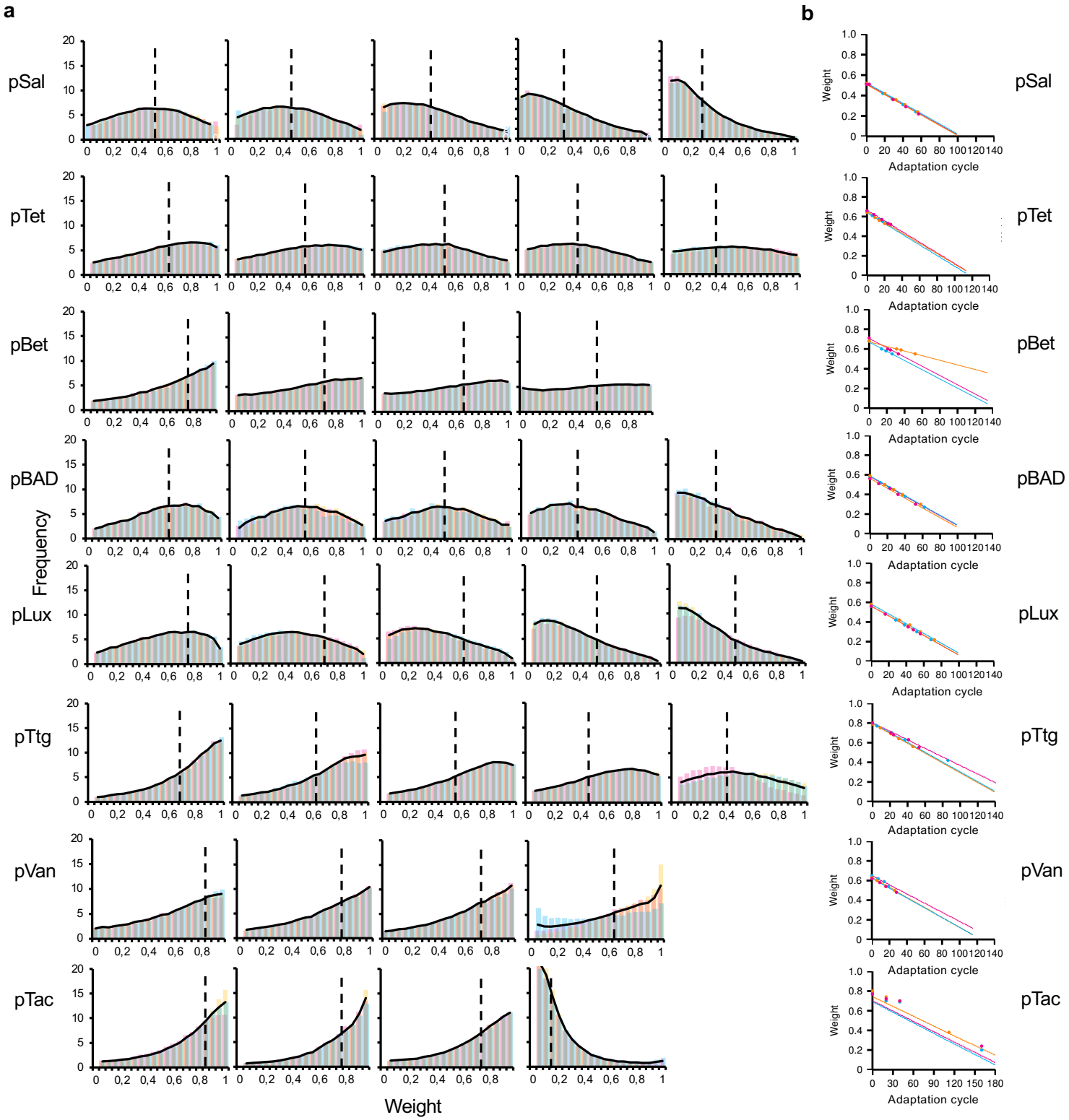

Extended Data Fig. 5. | AdaptoCell Adaptation measured by flow cytometry. a, Single-cell weight distribution for eight representative AdaptoCells analyzed via flow cytometry (see Methods) after each adaptation cycle, presented in three biological replicates (blue, pink, and yellow bars). The solid black line illustrates the average model prediction value for three replicates, with the vertical dashed line indicating the mean value. **b**, Model-predicted weights originating from a single clone for each biological replicate (Methods), with dots representing experimental data.

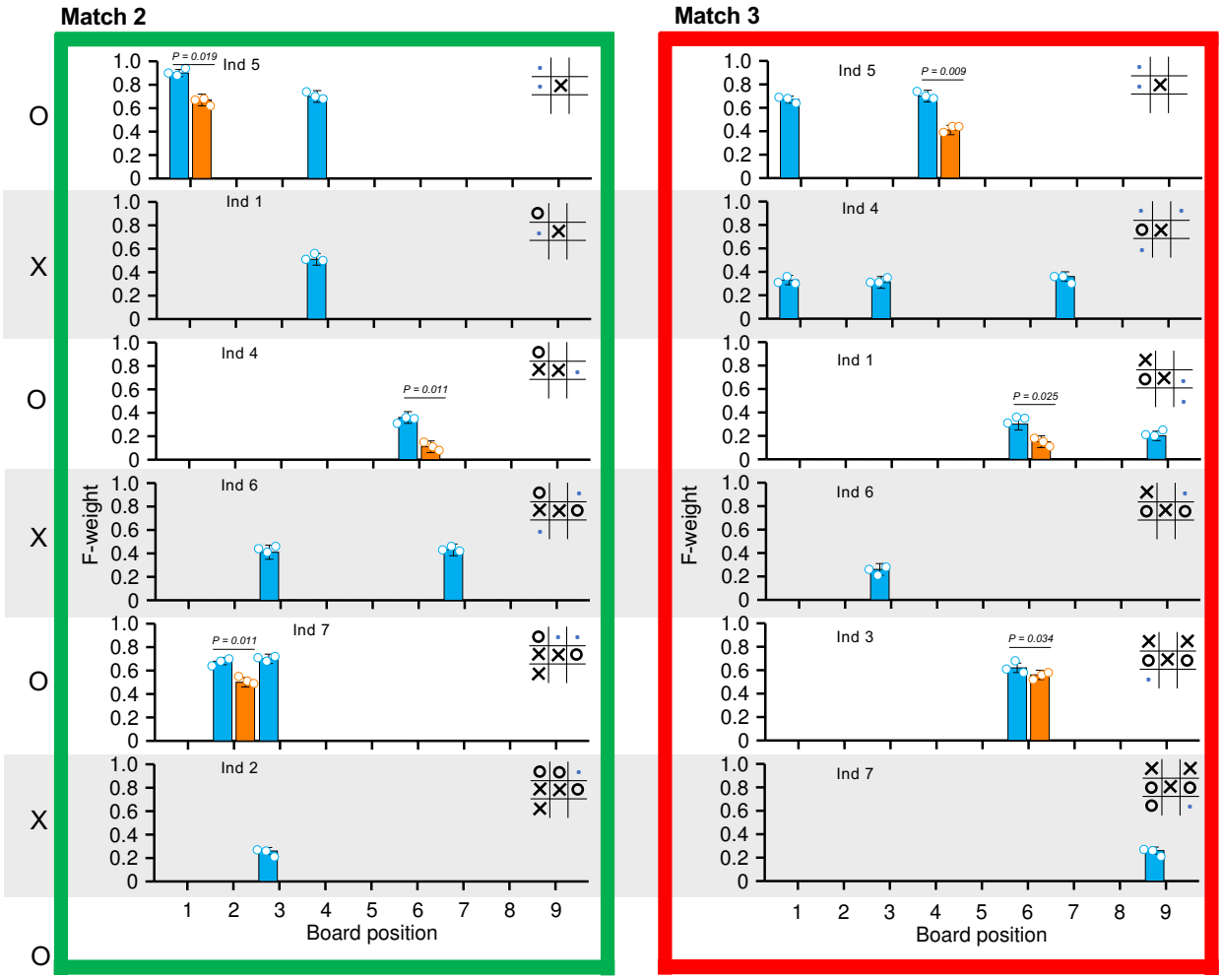

Extended Data Fig. 6. | Detail of the remaining adaptation from Fig. 4. Grey overlays align starting with the second overlay of Fig. 4e.

a **White stones (Player 1)**

Pos	Ind	AdaptoCell	Initial weight
1	4	pBAD	0.66 ± 0.04
2	8,9	pVan, pTac	0.82 ± 0.03, 0.77 ± 0.04
3	6,7,9	pCin, pTtg, pTac	0.61 ± 0.04, 0.72 ± 0.03, 0.75 ± 0.03
4	1	pSal	0.53 ± 0.05
6	3,7,8	pBet, pTtg, pVan	0.78 ± 0.05, 0.71 ± 0.05, 0.86 ± 0.04
7	2,6	pTet, pCin	0.67 ± 0.05, 0.65 ± 0.03
8	2,3,7,9	pTet, pBet, pTtg, pTac	0.66 ± 0.03, 0.80 ± 0.04, 0.73 ± 0.02, 0.77 ± 0.05
9	2,3,6,8	pTet, pBet, pCin, pVan	0.66 ± 0.03, 0.80 ± 0.04, 0.64 ± 0.02, 0.87 ± 0.03

Black stones (Player 2)

Pos	Ind	AdaptoCell	Initial weight
1	5	pLux	0.95 ± 0.03
2	3,4	pBet, pBAD	0.78 ± 0.03, 0.66 ± 0.04
3	2,7,8,9	pTet, pTtg, pVan, pTac	0.68 ± 0.03, ± 0.03, 0.87 ± 0.05, 0.77 ± 0.04
4	5	pLux	0.97 ± 0.01
6	1,2,4	pSal, pTet, pBAD	0.53 ± 0.05, 0.66 ± 0.03, 0.66 ± 0.04
7	3,6,7,8,9	pBet, pCin, pTtg, pVan, pTac	0.80 ± 0.04, 0.64 ± 0.03, 0.71 ± 0.03, 0.82 ± 0.03, 0.75 ± 0.03
8	1,2,4,6,7,9	pSal, pTet, pBAD, pCin, pTtg, pTac	0.53 ± 0.05, 0.67 ± 0.03, 0.66 ± 0.04, 0.64 ± 0.03, 0.61 ± 0.03, 0.73 ± 0.05
9	1,3,6,8	pSal, pBet, pCin, pVan	0.57 ± 0.03, 0.80 ± 0.03, 0.62 ± 0.05, 0.87 ± 0.04

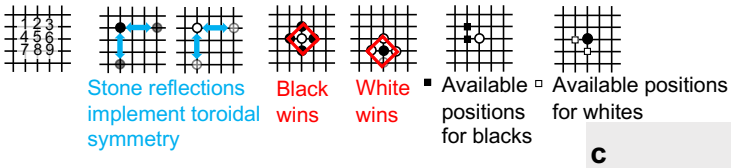

b **Match 1**

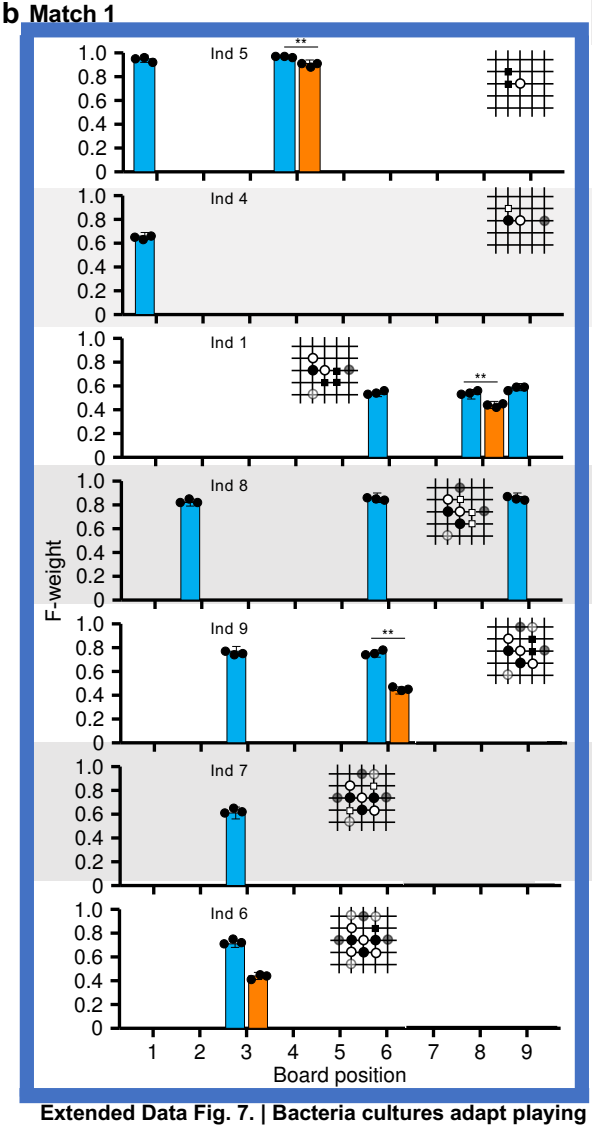

c

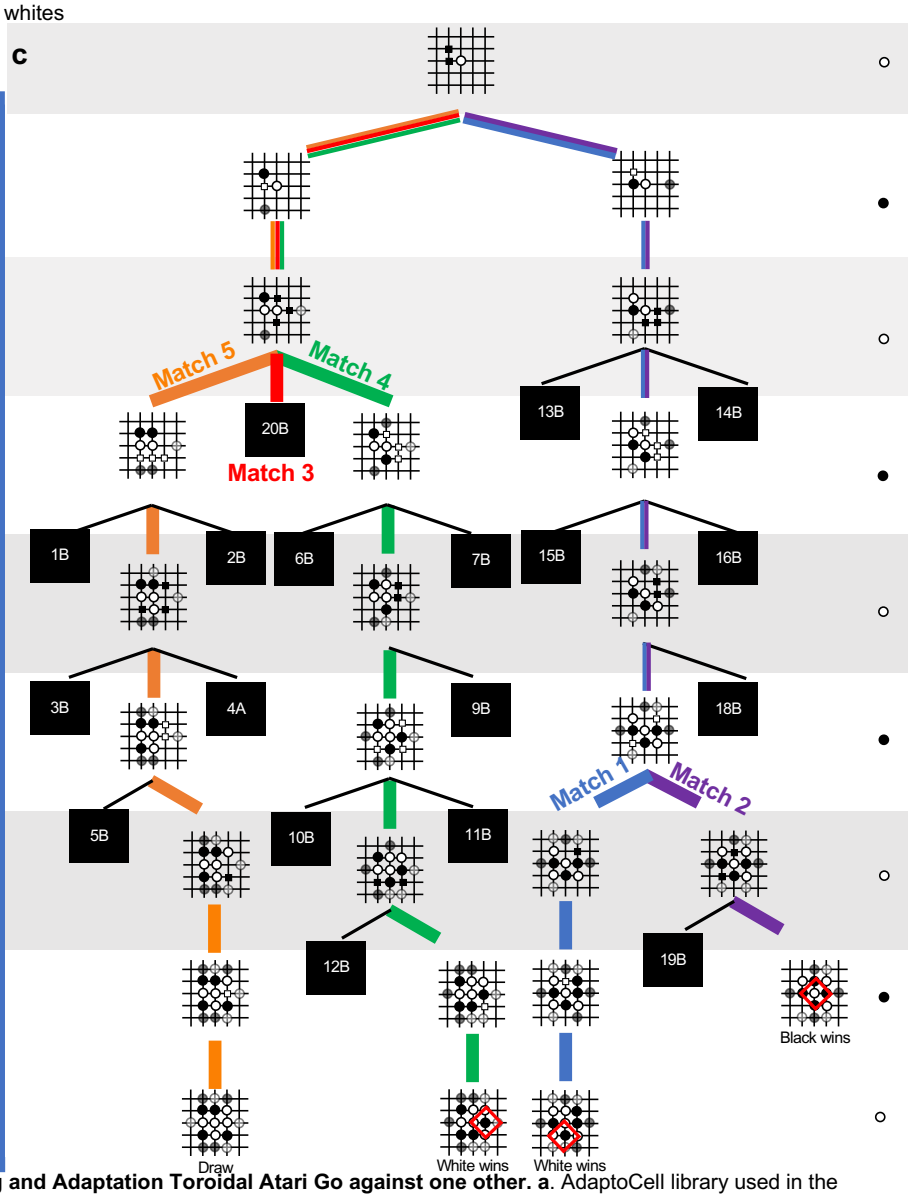

Extended Data Fig. 7. | Bacteria cultures adapt playing and Adaptation Toroidal Atari Go against one other. a. AdaptoCell library used in the bacterial cultures at each position (pos) with several AdaptoCell types per position. Bacteria play and adapt against each other according to the decision tree in panel **c**. Weights were measured before adaptation as F-weights and by DNA sequencing. Stone reflections implement the toroidal symmetry by replicating the stones to all equivalent positions (positions differing by 3 rows or columns). A player triumphs by 'surrounding' an opponent's stone with their stones or replicas. **b,** Loss of the bacteria first player (white stones) leads to adaptation with kanamycin (normalised mCherry fluorescence fraction before (blue) and after (orange) negative reinforcement Adaptation (± s.d. for n = 3)). **c,** Game decision tree, with black boxes indicating collapsed branches. Coloured branches indicate the losses used as training steps for either player.

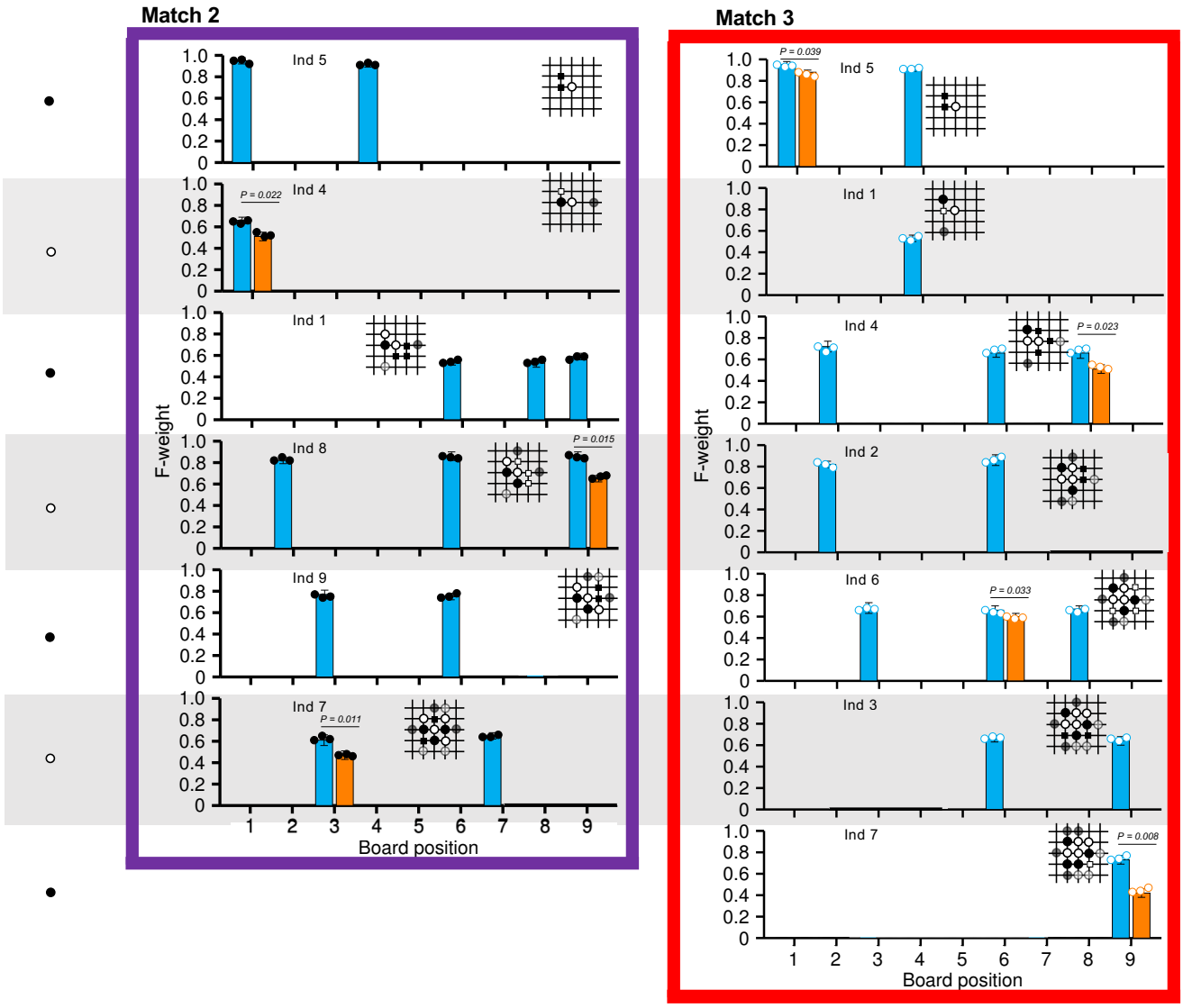

Extended Data Fig. 8. | Extended Data Fig. 7 continued. Matches 2 and 3 of the tournament of Extended Data Fig. 7. Grey overlays align with the second overlay of Extended Data Fig. 7c.

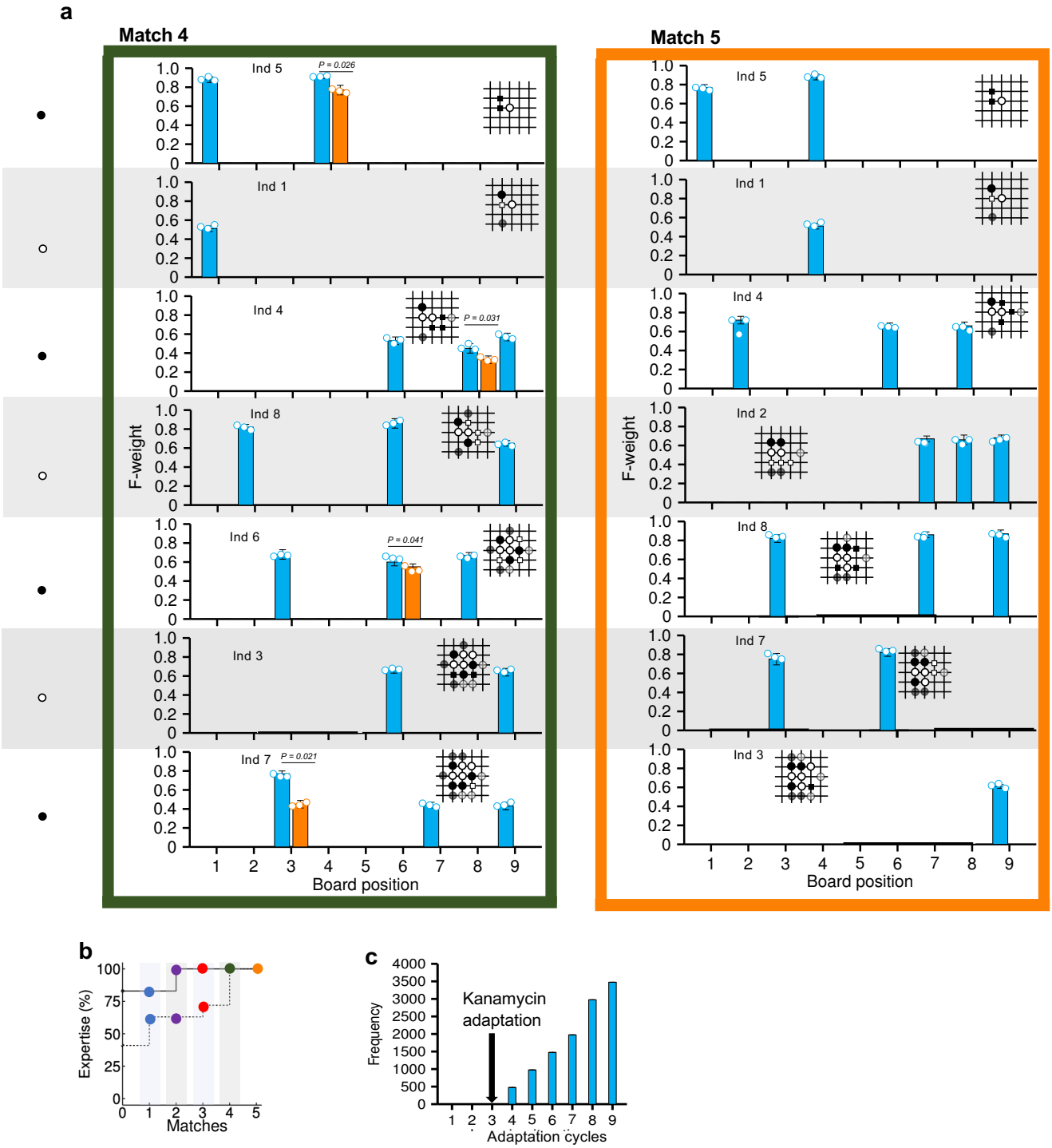

Extended Data Fig. 9. | Extended Data Fig. 7 continued. a, Matches 5 and 6 of the tournament of Extended Data Fig. 7. Grey overlays align with the second overlay of Extended Data Fig. 7c. **b,** Evolution of the expertise during a tournament where both players are able to learn by kanamycin adaptation, with dotted line denoting player 2. Grey overlays indicate the moves of Player 1. **c,** Distribution of Adaptation rounds required to achieve mastery of a set of 10,000 simulations of tournaments where the adaptation uses randomised inducers (similarly to Fig. 1g).

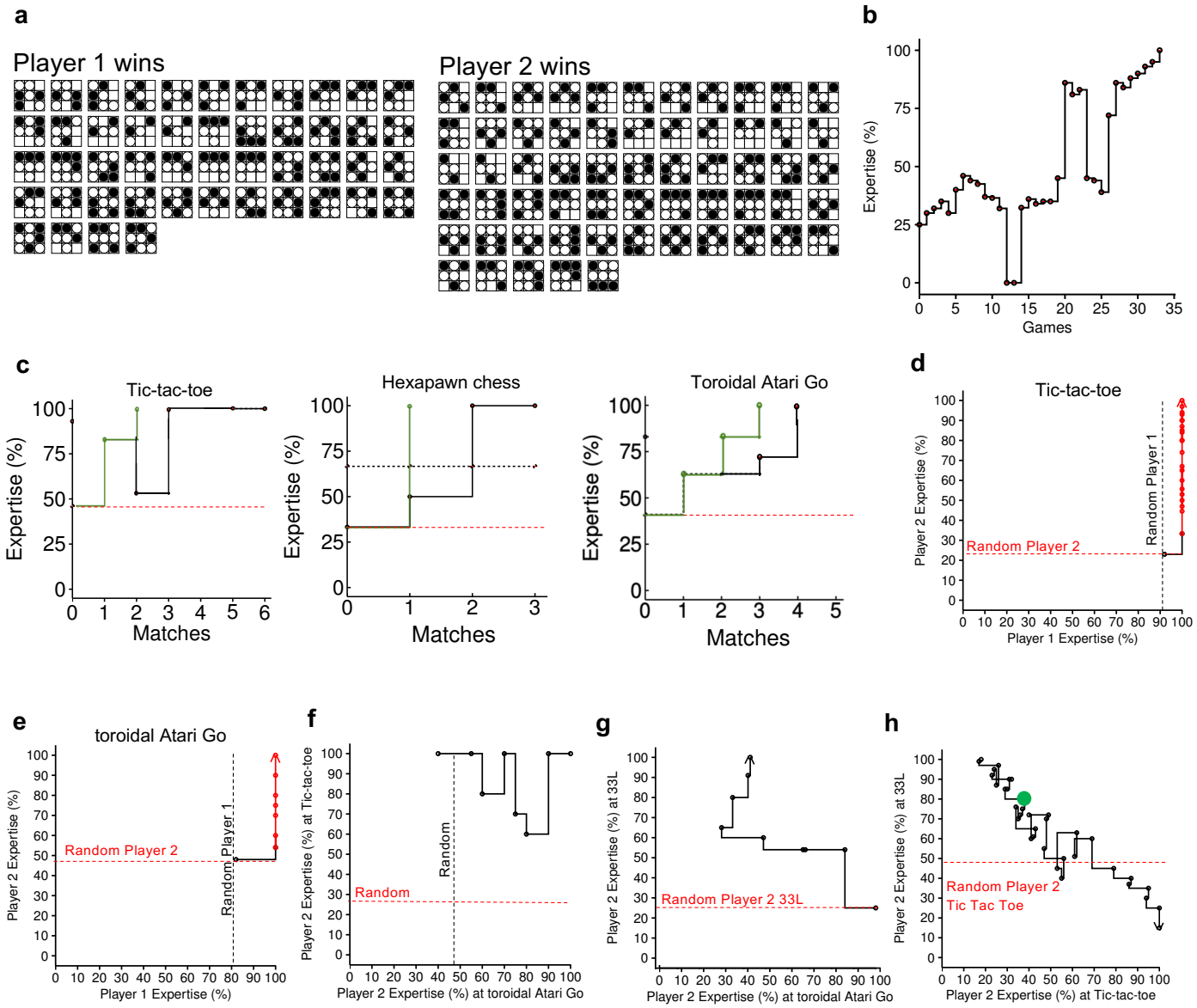

Extended Data Fig. 10 | Testing of the capabilities of a 9YES library to re-learn new games by computer simulations. a, Rules of the 33L game (the most difficult to learn). **b,** Evolution of the expertise of Player 2 during a tournament where both players are able to learn the 33L game by kanamycin adaptation. Dots indicate the expertise after kanamycin adaptation. **c,** Comparison of our reinforcement Adaptation (black) of Fig. 3, 4 and Ext. Data Fig. 7-9 against the fastest possible Adaptation (green) for the 3 games studied experimentally in the paper. **d,** Expertise evolution as both Player 1 (black) and Player 2 (red) at the game of Tic-tac-toe. **e,** Expertise evolution as both Player 1 (black) and Player 2 (red) at the game of Toroidal Atari Go after Adaptation the game of Tic-tac-toe. The expertise of Tic-tac-toe was maintained while achieving mastery of Atari Go. **g,** Expertise evolution as Player 2 at the 33L game at the expense of losing the expertise at Atari Go (and Tic-tac-toe). **h,** Re-training of the library to achieve back its mastery as Player 2 at the game of Tic-tac-toe. Green marker indicates the AdaptoCell fusion at match 9. See more details in Supplementary Text.

References

1. Lee, J.W. et al. Creating Single-Copy Genetic Circuits. *Molecular cell* **63**, 329-336 (2016).

2. Friedland, A.E. et al. Synthetic Gene Networks That Count. *Science* **324**, 1199-1202 (2009).

3. Regot, S. et al. Distributed biological computation with multicellular engineered networks. *Nature* **469**, 207-211 (2011).

4. Tamsir, A., Tabor, J.J. & Voigt, C.A. Robust multicellular computing using genetically encoded NOR gates and chemical 'wires'. *Nature* **469**, 212-215 (2011).

5. Moon, T.S. et al. Construction of a Genetic Multiplexer to Toggle between Chemosensory Pathways in Escherichia coli. *Journal of Molecular Biology* **406**, 215-227 (2011).

6. Shin, J., Zhang, S., Der, B.S., Nielsen, A.A.K. & Voigt, C.A. Programming Escherichia coli to function as a digital display. *Molecular Systems Biology* **16**, e9401 (2020).

7. Chen, T., Ali Al-Radhawi, M., Voigt, C.A. & Sontag, E.D. A synthetic distributed genetic multi-bit counter. *iScience* **24**, 103526 (2021).

8. Yokobayashi, Y., Weiss, R. & Arnold, F.H. Directed evolution of a genetic circuit. *Proceedings of the National Academy of Sciences* **99**, 16587-16591 (2002).

9. Isalan, M. et al. Evolvability and hierarchy in rewired bacterial gene networks. *Nature* **452**, 840-845 (2008).

10. Broedel, A.K., Jaramillo, A. & Isalan, M. Engineering orthogonal dual transcription factors for multi-input synthetic promoters. *Nature Communications* **7**, 13858 (2016).

11. Haseltine, E.L. & Arnold, F.H. Synthetic Gene Circuits: Design with Directed Evolution. *Annu Rev Biophys Biomol Struct* **36**, 1-19 (2007).

12. Nielsen, A.A.K. et al. Genetic circuit design automation. *Science* **352**, aac7341 (2016).

13. Du, P. et al. De novo design of an intercellular signaling toolbox for multi-channel cell-cell communication and biological computation. *Nature Communications* **11**, 4226 (2020).

14. Macdonald, J. et al. Medium scale integration of molecular logic gates in an automaton. *Nano letters* **6**, 2598-2603 (2006).

15. Sarpeshkar, R. Analog synthetic biology. *Phil. Trans. R. Soc. A* **372**, 20130110-20130122 (2014).

16. Daniel, R., Rubens, J.R., Sarpeshkar, R. & Lu, T.K. Synthetic analog computation in living cells. *Nature* **497**, 619-623 (2013).

17. Cherry, K.M. & Qian, L. Scaling up molecular pattern recognition with DNA-based winner-take-all neural networks. *Nature* **559**, 370-376 (2018).

18. Carrera, J., Elena, S.F. & Jaramillo, A. Computational design of genomic transcriptional networks with adaptation to varying environments. *Proceedings of the National Academy of Sciences of the United States of America* **109**, 15277-15282 (2012).

19. Didovyk, A. & Tsimring, L.S. Synthetic Gene Circuits Learn to Classify. *Cell Syst* **4**, 151-153 (2017).

20. Kanakov, O. et al. Multi-Input Distributed Classifiers for Synthetic Genetic Circuits. *PLoS ONE* **10**, e0125144-0125117 (2015).

21. Pei, R., Matamoros, E., Liu, M., Stefanovic, D. & Stojanovic, M.N. Training a molecular automaton to play a game. *Nature nanotechnology* **5**, 773-777 (2010).

22. Qian, L., Winfree, E. & Bruck, J. Neural network computation with DNA strand displacement cascades. *Nature* **475**, 368-372 (2011).

23. Banda, P., Teuscher, C. & Stefanovic, D. Training an asymmetric signal perceptron through reinforcement in an artificial chemistry. *Journal of The Royal Society Interface* **11**, 20131100 (2014).

24. Lin, X. et al. All-optical machine learning using diffractive deep neural networks. *Science* **361**, 1004-1008 (2018).

25. Pandi, A. et al. Metabolic perceptrons for neural computing in biological systems. *Nature Communications* **10**, 3880 (2019).

26. Li, X. et al. Synthetic neural-like computing in microbial consortia for pattern recognition. *Nature Communications* **12**, 3139 (2021).

27. Sarkar, K., Bonnerjee, D., Srivastava, R. & Bagh, S. A single layer artificial neural network type architecture with molecular engineered bacteria for reversible and irreversible computing. *Chemical Science* **12**, 15821-15832 (2021).

28. Tang, W. & Liu, D.R. Rewritable multi-event analog recording in bacterial and mammalian cells. *Science* **360**, eaap8992 (2018).

29. Schrittwieser, J. et al. Mastering Atari, Go, chess and shogi by planning with a learned model. *Nature* **588**, 604-609 (2020).

30. Rodriguez-Beltran, J. et al. Multicopy plasmids allow bacteria to escape from fitness trade-offs during evolutionary innovation. *Nat Ecol Evol* **2**, 873-881 (2018).

31. Aryaman, J., Johnston, I.G. & Jones, N.S. Mitochondrial Heterogeneity. *Frontiers in Genetics* **9**, 718 (2019).

562 32. Prakash, S., Racovita, A., Petrucci, T., Galizi, R. & Jaramillo, A. qSanger:
563 Quantification of genetic variants in bacterial cultures by Sanger sequencing.
564 *BioDesign Research* **0** (2023).

565 33. Chua, L. Memristor-The missing circuit element. *IEEE Transactions on Circuit Theory*
566 **18**, 507-519 (1971).

567 34. Shen, S. et al. Dynamic signal processing by ribozyme-mediated RNA circuits to
568 control gene expression. *Nucleic Acids Research* **43**, 5158-5170 (2015).

569 35. Summers, D. The Biology of Plasmids. (John Wiley & Sons, 2009).

570 36. Raman, S., Rogers, J.K., Taylor, N.D. & Church, G.M. Evolution-guided optimization
571 of biosynthetic pathways. *Proceedings of the National Academy of Sciences* **111**,
572 17803-17808 (2014).

573 37. Tolia, N.H. & Joshua-Tor, L. Strategies for protein coexpression in Escherichia coli.
574 *Nature methods* **3**, 55-64 (2006).

575 38. Black, J. & Vos, J.M. Establishment of an oriP/EBNA1-based episomal vector
576 transcribing human genomic beta-globin in cultured murine fibroblasts. *Gene Ther* **9**,
577 1447-1454 (2002).

578 39. Beal, J. et al. Model-Driven Engineering of Gene Expression from RNA Replicons.
579 *ACS Synthetic Biology* **4**, 48-56 (2015).

580 40. Ibba, M., Kast, P. & Hennecke, H. Substrate specificity is determined by amino acid
581 binding pocket size in Escherichia coli phenylalanyl-tRNA synthetase. *Biochemistry*
582 **33**, 7107-7112 (1994).

583 41. Jaramillo, A. Engineered stable ecosystems. *Nat Microbiol* **2**, 17119 (2017).

584 42. San Millan, A., Escudero, J.A., Gifford, D.R., Mazel, D. & Maclean, R.C. Multicopy
585 plasmids potentiate the evolution of antibiotic resistance in bacteria. *Nat Ecol Evol* **1**,
586 10 (2016).

587 43. Fodale, V., Pierobon, M., Liotta, L. & Petricoin, E. Mechanism of cell adaptation: when
588 and how do cancer cells develop chemoresistance? *Cancer J* **17**, 89-95 (2011).

589 44. Stojanovic, M.N. & Stefanovic, D. A deoxyribozyme-based molecular automaton.
590 *Nature biotechnology* **21**, 1069-1074 (2003).

591 45. Elo, A.E. The rating of chessplayers, past and present. (BT Batsford Limited, 1978).

592 46. Gardner, M. Mathematical games. *Scientific American* **232**, 126 (1958).

593 47. Cobb, W.S. The book of GO. (Sterling Publishing Company, Inc., 2002).

594 48. Liu, X. et al. De novo design of programmable inducible promoters. *Nucleic Acids*
595 *Research* **47**, 10452-10463 (2019).

596 49. Garruss, A.S., Collins, K.M. & Church, G.M. Deep representation learning improves
597 prediction of LacI-mediated transcriptional repression. *Proceedings of the National*
598 *Academy of Sciences* **118**, e2022838118 (2021).

599 50. Engel, A. & Van den Broeck, C. Statistical Mechanics of Learning. (Cambridge
600 University Press, 2012).

601 51. Rizik, L., Danial, L., Habib, M., Weiss, R. & Daniel, R. Synthetic neuromorphic
602 computing in living cells. *Nature Communications* **13**, 5602 (2022).

603 52. Maass, W. On the computational power of winner-take-all. *Neural Comput* **12**, 2519-
604 2535 (2000).

605 53. Krotov, D. & Hopfield, J.J. Unsupervised learning by competing hidden units.
606 *Proceedings of the National Academy of Sciences* **116**, 7723-7731 (2019).

607 54. Guet, C.C., Elowitz, M.B., Hsing, W. & Leibler, S. Combinatorial synthesis of genetic
608 networks. *Science* **296**, 1466-1470 (2002).

609 55. Xie, Z., Wroblewska, L., Prochazka, L., Weiss, R. & Benenson, Y. Multi-Input RNAi-
610 Based Logic Circuit for Identification of Specific Cancer Cells. *Science* **333**, 1307-1311
611 (2011).

612 56. Kong, W., Meldgin, D.R., Collins, J.J. & Lu, T. Designing microbial consortia with
613 defined social interactions. *Nature chemical biology* **14**, 821-829 (2018).

614 57. Mathis, R. & Ackermann, M. Response of single bacterial cells to stress gives rise to
615 complex history dependence at the population level. *Proceedings of the National*
616 *Academy of Sciences of the United States of America* **113**, 4224-4229 (2016).

617 58. St-Pierre, F. et al. in ACS Synthetic Biology, Vol. 2 537-541 (American Chemical
618 Society, 2013).

619 59. Gibson, D.G. et al. Enzymatic assembly of DNA molecules up to several hundred
620 kilobases. *Nature methods* **6**, 343-345 (2009).

621 60. Martínez-García, E. et al. SEVA 3.0: an update of the Standard European Vector
622 Architecture for enabling portability of genetic constructs among diverse bacterial
623 hosts. *Nucleic Acids Research* **48**, D1164-D1170 (2020).

624 61. Chen, Y.-J. et al. Characterization of 582 natural and synthetic terminators and
625 quantification of their design constraints. *Nature methods* **10**, 659-664 (2013).

626 62. Lin-Chao, S., Chen, W.T. & Wong, T.T. High copy number of the pUC plasmid results
627 from a Rom/Rop-suppressible point mutation in RNA II. *Molecular microbiology* **6**,
628 3385-3393 (1992).

629 63. Camps, M. Modulation of ColE1-like plasmid replication for recombinant gene
630 expression. *Recent Pat DNA Gene Seq* **4**, 58-73 (2010).

631 64. Lou, C., Stanton, B., Chen, Y.-J., Munsky, B. & Voigt, C.A. Ribozyme-based insulator
632 parts buffer synthetic circuits from genetic context. *Nature biotechnology* **30**, 1137-
633 1142 (2012).

634 65. Shaner, N.C. et al. Improved monomeric red, orange and yellow fluorescent proteins
635 derived from Discosoma sp. red fluorescent protein. *Nature biotechnology* **22**, 1567-
636 1572 (2004).

637 66. Krell, T. et al. Optimization of the palindromic order of the TtgR operator enhances
638 binding cooperativity. *Journal of Molecular Biology* **369**, 1188-1199 (2007).

639 67. Gitzinger, M. et al. The food additive vanillic acid controls transgene expression in
640 mammalian cells and mice. *Nucleic Acids Research* **40**, e37-e37 (2012).

641 68. Meyer, A.J., Segall-Shapiro, T.H., Glassey, E., Zhang, J. & Voigt, C.A. Escherichia coli
642 "Marionette" strains with 12 highly optimized small-molecule sensors. *Nature chemical*
643 *biology* **15**, 196-204 (2019).

644 69. Cock, P.J.A. et al. Biopython: freely available Python tools for computational molecular
645 biology and bioinformatics. *Bioinformatics* **25**, 1422-1423 (2009).

646 70. Cermak, N., Datta, M.S. & Conwill, A. Rapid, Inexpensive Measurement of Synthetic
647 Bacterial Community Composition by Sanger Sequencing of Amplicon Mixtures.
648 *iScience* **23**, 100915 (2020).
649

650